



This is a repository copy of *Global wildfire patterns and drivers under climate change*.

White Rose Research Online URL for this paper:

<https://eprints.whiterose.ac.uk/id/eprint/235894/>

Version: Published Version

---

**Article:**

Bhattarai, H. [orcid.org/0000-0002-7132-6660](https://orcid.org/0000-0002-7132-6660), Val Martin, M. [orcid.org/0000-0001-9715-0504](https://orcid.org/0000-0001-9715-0504), Sitch, S. et al. (2 more authors) (2025) Global wildfire patterns and drivers under climate change. *Biogeosciences*, 22 (23). pp. 7591-7610. ISSN: 1726-4170

<https://doi.org/10.5194/bg-22-7591-2025>

---

**Reuse**

This article is distributed under the terms of the Creative Commons Attribution (CC BY) licence. This licence allows you to distribute, remix, tweak, and build upon the work, even commercially, as long as you credit the authors for the original work. More information and the full terms of the licence here:

<https://creativecommons.org/licenses/>

**Takedown**

If you consider content in White Rose Research Online to be in breach of UK law, please notify us by emailing [eprints@whiterose.ac.uk](mailto:eprints@whiterose.ac.uk) including the URL of the record and the reason for the withdrawal request.



[eprints@whiterose.ac.uk](mailto:eprints@whiterose.ac.uk)  
<https://eprints.whiterose.ac.uk/>



# Global wildfire patterns and drivers under climate change

Hemraj Bhattarai<sup>1,a</sup>, Maria Val Martin<sup>2</sup>, Stephen Sitch<sup>3</sup>, David H. Y. Yung<sup>1</sup>, and Amos P. K. Tai<sup>1,4</sup>

<sup>1</sup>Department of Earth and Environmental Sciences, Faculty of Science, The Chinese University of Hong Kong, Hong Kong, China

<sup>2</sup>Leverhulme Centre for Climate Change Mitigation, School of Biosciences, University of Sheffield, Sheffield, UK

<sup>3</sup>Faculty of Environment, Science and Economy, University of Exeter, Exeter, UK

<sup>4</sup>State Key Laboratory of Agrobiotechnology and Institute of Environment, Energy and Sustainability, The Chinese University of Hong Kong, Hong Kong, China

<sup>a</sup>currently at: Division of Environment and Sustainability, the Hong Kong University of Science and Technology, Hong Kong, China

**Correspondence:** Maria Val Martin (m.valmartin@sheffield.ac.uk) and Amos P. K. Tai (amostai@cuhk.edu.hk)

Received: 21 February 2025 – Discussion started: 5 March 2025

Revised: 6 November 2025 – Accepted: 15 November 2025 – Published: 3 December 2025

**Abstract.** Wildfires increasingly threaten human lives, ecosystems, and climate, yet a comprehensive understanding of the factors driving their future dynamics and emissions remains elusive, hampering mitigation efforts. In this study, we assessed how future climate change would influence global burned area (BA) and carbon emissions between 2015 to 2100 using the Community Land Model version 5 (CLM5) with active biogeochemistry and fires. The model reasonably captures observed spatial and seasonal patterns of BA and emissions during the present-day reference period. Under two future scenarios – SSP1-2.6 (low warming) and SSP3-7.0 (high warming) – CLM5 projects global BA increases of +6400 and +7500 km<sup>2</sup> yr<sup>-1</sup>, respectively. Northern extratropics, particularly the boreal regions, emerge as the dominant hotspot with BA increasing by 200 % and fire-related carbon emissions by +4 to +7 Tg yr<sup>-1</sup>, while in tropical regions BA remains comparatively stable or slightly declines. These shifts are associated with warming-induced changes in vegetation productivity and fuel dryness, particularly in boreal ecosystems. Enhanced vegetation carbon contributes to fuel availability, while declines in relative humidity and soil moisture increase flammability. Elevated atmospheric CO<sub>2</sub> also contributes to these effects by enhancing biomass growth through fertilization and increasing water use efficiency, thereby affecting fire risks and carbon emissions. These findings underscore the need to integrate climate-vegetation-fire interactions into global policy frame-

works for effective mitigation and adaptation planning of future fire-related threats.

## 1 Introduction

Wildfires, known for their unplanned and rapid spread, have profound and wide-ranging impacts, from threatening human welfare and infrastructure to altering ecosystems and contributing to global climate dynamics (Li et al., 2017; Bowman et al., 2020). These events cause devastation through combustion and release of vast amounts of chemically and radiatively active gases and aerosols into the atmosphere (Andreae and Merlet, 2001; Bowman et al., 2009; Coen et al., 2013; Liu et al., 2019; Tang et al., 2022; Zhang et al., 2022; Bhattarai et al., 2024). Annually, wildfires consume millions of square kilometers of land, shaping natural forest successions while disrupting ecological equilibria (Wright and Heinzelman, 2014). Recent estimates on Global Fire Emissions Database version five (GFED5) shows a declining trend (1.21 % yr<sup>-1</sup>) of global annual burned area (BA) from 2001 to 2020, with a 20-year average BA of 7.74 million km<sup>2</sup> yr<sup>-1</sup>, which is around 5.9 % of ice free land (Chen et al., 2023a). Such decline is primarily driven by reduced BA in savannas, mainly due to agricultural expansion and intensification (Andela et al., 2017). However, BA trends largely vary with region, where the boreal region experiences an increasing trend (2.5 % yr<sup>-1</sup>), while most other regions show reductions by

up to  $2.7\% \text{ yr}^{-1}$  (Chen et al., 2023a). BA declines over vast grasslands but increases in small forested areas, resulting in a sharp overall reduction in BA, while carbon emissions remain nearly stable, as forests emit more carbon per unit area than grasslands, offsetting the decline in emissions (Zheng et al., 2021). Long-term analysis indicates that climate change may exacerbate BA trends, substantially increasing carbon emissions from the biosphere and amplifying disruptions to the global carbon cycle (van der Werf et al., 2010; Burton et al., 2024b; Jones et al., 2024).

The socioeconomic impacts of wildfires are also substantial (Kochi et al., 2010; Tymstra et al., 2020). For instance, the 2019/2020 Australian wildfires resulted in nearly USD 100 billion of economic losses including firefighting costs and damage to infrastructure, business, and wildlife (Roach, 2020). Similar devastating events in Canada peaked in 2023 due to a combination of hot, dry weather conditions and human activities, including vehicle accidents, recreational uses of forests, and land management practices, causing accidental ignitions (Owens, 2023; Byrne et al., 2024). Lightning is the major igniting source of wildfires in Canada, contributing to 85 % of the total burned area every year. Additionally, unprecedented wildfires have ravaged the western US (Higuera and Abatzoglou, 2021), Siberia (Bondur et al., 2020), and the Himalayas (Bhattarai et al., 2023), often exacerbated by climate change-associated weather anomalies (Jones et al., 2022).

Wildfire dynamics is governed by the complex interplay of natural and human factors. Meteorological variables, such as temperature, soil moisture, precipitation, wind, and relative humidity (RH) significantly influence fuel availability and combustibility (Aldersley et al., 2011; Kloster et al., 2012; Hantson et al., 2015; Knorr et al., 2016; Jones et al., 2022; Senande-Rivera et al., 2022; Shi and Touge, 2022). Higher temperatures and stronger winds increase wildfire risks, while precipitation and soil moisture mitigate fire spread. Vegetation dynamics also play a critical role, as elevated precipitation and  $\text{CO}_2$  levels enhance vegetation growth, which in turn can potentially increase the availability of combustible materials (Allen et al., 2024). In addition, anthropogenic land use changes, including deforestation and agricultural expansion, have transformed landscapes in ways that either amplify or suppress wildfire risks. For example, agricultural expansion in South America has reduced BA in some regions (Aldersley et al., 2011; Zubkova et al., 2023). These factors collectively drive the spatiotemporal variability of wildfires.

Climate change is a dominant driver of increasing wildfire risks, with rising global temperatures and more frequent El Niño–Southern Oscillation (ENSO) events leading to regional temperature extremes and prolonged dry periods (Fuller and Murphy, 2006; Fasullo et al., 2018). These conditions exacerbate wildfire frequency and intensity, particularly in boreal and tropical forests (IPCC, 2014; Fasullo et al., 2018). For instance, Canadian fire season has extended

by around two weeks, starting a week earlier and ending a week later compared to its pattern 50 years before (Owens, 2023). Future projections indicate heightened wildfire risks due to climate-induced shifts in meteorological conditions, such as snow melt timing and extended droughts (Flannigan et al., 2009; Liu et al., 2010; Veira et al., 2016; Di Virgilio et al., 2019; Li et al., 2020; Jones et al., 2022). However, the interplay of socioeconomic factors, including population density and gross domestic product (GDP), may mitigate these risks through improved fire suppression and management measures (Kloster et al., 2012; Val Martin et al., 2015; Veira et al., 2016). Studies based on Representative Concentration Pathways (RCPs) suggest that while climate change amplifies fire risks, human intervention could counterbalance these effects to some extent (Dong et al., 2022; Nurrohmam et al., 2024).

Despite these advancements, significant knowledge gaps remain in understanding the divergent fire dynamics over tropics and boreal regions, their seasonal variability, and the roles of vegetation and hydrological changes under future climate conditions. While several studies have projected future wildfire trends and carbon emissions using various climate scenarios (e.g., Scholze et al., 2006; Knorr et al., 2016; Kloster and Lasslop, 2017; Wu et al., 2022), research specifically addressing the effects of recently developed low and high warming climate pathways on BA and wildfire emissions remains limited. Existing studies have primarily focused on fire weather indices (Quilcaille et al., 2023) or specific mitigation strategies such as solar geoengineering (Tang et al., 2023), leaving the broader influence of climate change on global wildfire patterns, independent of direct socioeconomic drivers, less explored. Investigating future fire dynamics using the latest climate-fire-enabled global terrestrial system model, combined with state-of-the-art climate projections, is essential to improve predictions of wildfire frequency and intensity and their cascading effects on air quality, carbon cycling, and climate feedback.

In this study, we examined how future climate change would impact global wildfires throughout the 21st century, focusing on SSP1-2.6 (low-warming) and SSP3-7.0 (high-warming) (hereafter referred to as SSP1 and SSP3). Using the climate projections from the Community Earth System Model (CESM) database, we analyzed trends in BA and emissions of key carbonaceous species – total carbon (TC), black carbon (BC), organic carbon (OC), and carbon monoxide (CO) – to provide new insights into the spatial distribution and intensity of future wildfire events. By focusing on SSP1/SSP3 climate-driven changes while holding socioeconomic drivers (land use and populations) constant, our study isolates the effects of warming on fire dynamics, offering a clearer understanding of how different climate pathways shape future wildfire risks. This research highlights the potential implications for carbon emissions and informs strategies to mitigate the impacts of future wildfires in a changing climate.

## 2 Methods

### 2.1 Community Land Model (CLM)

In this study, we used the Community Land Model version 5 (CLM5), the land component within the Community Earth System Model (CESM) (Lawrence et al., 2019; Danabasoglu et al., 2020). CLM5 was run with active biogeochemistry and an interactive fire module (Li et al., 2013) to investigate the implications of climate change on wildfires and their resulting effects on BA and emissions of carbonaceous species. This configuration enables vegetation to respond dynamically to changes in climate conditions and elevated CO<sub>2</sub> levels within its carbon and nitrogen cycles. CLM5 operates at the plant functional type (PFT) level, simulating interactions among each PFT, soil organic matter, and atmosphere, thereby capturing the impacts of climate change and fires on terrestrial ecosystems. While CLM5 simulates vegetation structure, carbon allocation, and biomass dynamics in response to environmental drivers, it does not include dynamic changes in PFT composition, competition, or succession as in Dynamic Global Vegetation Models. This constraint may limit the representation of biome shifts and their long-term feedbacks on fire regimes. Thus, vegetation types remain fixed in space, although their biomass and productivity evolve, which is important for fire regime responses driven by vegetation.

We conducted model simulations at a horizontal grid resolution of  $0.9^\circ \times 1.25^\circ$  (latitude  $\times$  longitude). Within each grid cell, subgrid cells defining various land cover types in CLM5 are represented, including urban, glacier, and vegetated areas. Vegetated land is further characterized by 16 distinct PFTs, encompassing diverse vegetation ranging from forest to grasslands and crops, and including bare land.

### 2.2 Fire module in CLM5

The CLM5 fire module has been rigorously validated through comparisons with fire emission inventories and satellite observations, and has been widely adopted in prior research (Li et al., 2012, 2013, 2017; Ford et al., 2018; Li et al., 2019; Tang et al., 2023). The CLM5 fire module represents an advancement in understanding the interplay among fire dynamics, vegetation, and the Earth's climate system (Li et al., 2013). Built on a process-based fire parameterization, the CLM5 fire module accounts for four distinct fire types: (i) agricultural fires in croplands, (ii) deforestation fires in tropical closed forests, (iii) peat fires, and (iv) non-peat fires occurring beyond croplands and tropical closed forests (Li et al., 2012, 2013). Fire ignitions include both natural and anthropogenic sources, with lightning datasets from NASA serving as the basis for natural ignitions, while anthropogenic ignitions are influenced by population density and GDP, whereby higher population and GDP effectively suppress fire occurrences. The module estimates the likelihood of fire oc-

currence by considering the availability of biomass as fuel, combustibility of the fuel depending on its moisture content, and presence of an ignition source, whether human-induced or from lightning. Thus, BA within the CLM5 fire scheme is driven by socioeconomic activities, vegetation composition, and prevailing weather conditions (e.g., temperature, RH, wind, precipitation, and soil moisture). Upon determination of BA, gas and aerosol emissions from fires are obtained at the grid cell level.

In this study, to focus on the impacts of future climate change on wildfires, land use and populations were held constant at present-day levels, allowing only climate to evolve over time. This introduces a partial decoupling from the SSP framework but allows us to attribute changes in BA and emissions directly to climate-driven factors, independent of socioeconomic and land use shifts. While fixing land use change directly affects fuel availability, fixing population change is associated with fire management (suppress or ignite), thereby affecting BA and carbon emissions. This approach thus fixes natural and anthropogenic ignition sources while permitting fuel availability and combustibility to change along with future climate. Climate change accounts for changes in CO<sub>2</sub> levels and precipitation, temperature, pressure, RH, wind, and radiation. These changes exert direct influences on fuel availability and combustibility, shaped by evolving climate conditions and vegetation characteristics. Although CLM5 tracks four fire types, our analysis focuses on total BA and aggregated emissions. Since land use and populations were held constant in our simulations, the projected increases in BA are primarily attributable to natural vegetation and peat fires, particularly dominant in high-latitude regions. We considered two future climate projections: low warming (SSP1-2.6; hereafter referred to as SSP1) and high warming (SSP3-7.0; hereafter referred to as SSP3). SSP1 projects an increase of atmospheric CO<sub>2</sub> of 70 ppm up to 2050, after which it stabilizes, whereas SSP3 projects a 140 ppm increase by 2050 and 467 ppm by 2100, relative to 2015 levels (400 ppm). Global land temperature rises sharply under SSP3, with an increase of 1.6 °C during the 2050s (2050–2059 average) and 3.8 °C during the 2090s (2090–2099 average) compared to present-day conditions (2015–2024 average of 10.4 °C). In contrast, SSP1 shows a temperature increase of only 1.2 °C by 2050, with relatively stable conditions in the later part of the century.

### 2.3 Model experiments

We first spun up CLM5 with the fire module active to steady state in 1850 using an accelerated decomposition procedure and fixed pre-industrial CO<sub>2</sub>, land use, and atmospheric nitrogen (N) deposition (Lawrence et al., 2019). The accelerated decomposition spin-up was for about 1200 years as the total soil organic matter carbon in the Arctic regions required a longer time frame to reach equilibrium; we considered the model fully spun up when the land surface had more

than 97 % of the total ecosystem carbon in equilibrium. The present-day spin-up was based on a historical simulation for 1850–2014 using historical N and aerosol deposition, atmospheric CO<sub>2</sub> forcing, land use change, and meteorological forcings from the Global Soil Wetness Project (GSWP3v1) (Lawrence et al., 2019).

For future runs, we initialized CLM5 in 2015 with the prescribed climate for the low and high warming scenarios simulated by CESM2 for Coupled Model Intercomparison Project Phase 6 (CMIP6), and conducted transient simulations until 2100. Both SSP1 and SSP3 were forced with outputs from the same CESM ensemble member, meaning that they share internal variability in the early part of the simulation. For the first ten years, both scenarios exhibit very similar behavior in terms of BA (SSP1:  $5.18 \pm 0.37$  million km<sup>2</sup>, SSP3:  $5.15 \pm 0.39$  million km<sup>2</sup>) and emissions (Fig. S1 in the Supplement), as climate and CO<sub>2</sub> levels at the start of both scenarios are nearly identical and have not yet diverged. Therefore, we considered the period from 2015 to 2024 for SSP1 as representative of present-day conditions (referred to as “Baseline” and reported average  $\pm$  standard deviation, SD). Although these are transient simulations, for certain analyses, we selected results from 2090 to 2099 (referred to as “2090s” and reported average  $\pm$  SD) to calculate the differences from the present-day conditions for the respective climate scenario to estimate future changes. To analyze long-term trends, we applied a centered 30-year moving average to the annual values, which was implemented using a symmetric padding method with convolution, ensuring that each smoothed value is centered on the corresponding year. These smoothing highlights decadal variability and long-term trends while minimizing short-term fluctuations. These experiments were aimed to assess the isolated impacts of climate change on wildfires and emissions of air pollutants, while holding anthropogenic land management constant.

## 2.4 Machine learning models

To assess the relative contribution of climate and vegetation drivers to high latitudes ( $\geq 40^\circ$  N) summer (JJA) BA, we trained three supervised machine learning models: XGBoost, LightGBM, and Random Forest. These models were trained on monthly grid cell-level data using predictors from CLM5 simulations: 10 cm soil moisture, total vegetation carbon (TOTVEGC), 2 m air temperature, 2 m RH, 10 m wind speed, precipitation, and climate water availability (CWA = precipitation – evapotranspiration).

Each model was trained using an 80/20 train-test split, with Bayesian hyperparameter optimization and 5-fold cross-validation. Predictive performance was assessed using the coefficient of determination ( $R^2$ ) and root mean square error (RMSE) on held-out test sets for both SSP1 and SSP3 scenarios. XGBoost demonstrated the best performance across both scenarios and was selected for fur-

**Table 1.** Performance metrics ( $R^2$  and RMSE) for XGBoost, LightGBM, and Random Forest models in predicting boreal summer burned area under SSP1 and SSP3 scenarios.

ML model	SSP1		SSP3	
	$R^2$	RMSE	$R^2$	RMSE
XGBoost	0.70	947.27	0.62	1106.13
LightGBM	0.59	1112.72	0.54	1215.03
Random Forest	0.52	1202.24	0.49	1284.20

ther interpretation (Table 1). To interpret the model outputs, we used both gain-based built-in feature importance and SHAP (Shapley Additive exPlanations) values to capture the marginal effects of each feature and their nonlinear interactions with BA.

To evaluate the realism of CLM5 fire drivers, we conducted a parallel analysis using GFED5 observed burned area (2007–2020) (Chen et al., 2023b) and ERA5-Land reanalysis data (Muñoz Sabater, 2019). The observational analysis used the same seven predictors, with leaf area index (LAI) serving as a proxy for vegetation carbon and top layer soil moisture (0–7 cm) serving equivalent to 10 cm CLM5 soil moisture. Both global and high latitudes domains were analyzed. Notably, the high latitude GFED5 dataset exhibits extreme zero-inflation, with only 5 % of spatiotemporal observations containing non-zero burned area during JJA, contributing to lower predictive performance ( $R^2 = 0.23$ ) compared to the global analysis ( $R^2 = 0.58$ ). This data limitation reflects the inherent challenge of predicting fire occurrence in observation-sparse boreal regions.

## 3 Results

### 3.1 Validation of global burned area and fire emissions

Our model results capture both the spatial distribution and magnitude of global BA and wildfire emissions (Fig. 1), demonstrating good agreement with the Global Fire Emission Database (GFED) (Randerson et al., 2017; Chen et al., 2023a). GFED derives estimates of BA and emissions by integrating satellite-derived fire activity data with biogeochemical modeling approaches. We consider both GFED4.1 and GFED5 in this validation as they use different methodologies, with GFED5 accounting for small fires that are often missed by satellite sensors, leading to higher BA estimates compared to GFED4.1 (Chen et al., 2023a).

For the present day (2015–2024), CLM5 simulates a global annual BA of  $5.18 \pm 0.37$  million km<sup>2</sup> (mean  $\pm$  SD), which lies between the estimates of GFED4.1 averaged for the 2007–2016 ( $4.48 \pm 0.36$  million km<sup>2</sup>) and GFED5 averaged for the 2011–2020 ( $7.31 \pm 0.39$  million km<sup>2</sup>). The decadal mean is calculated based on the data available in

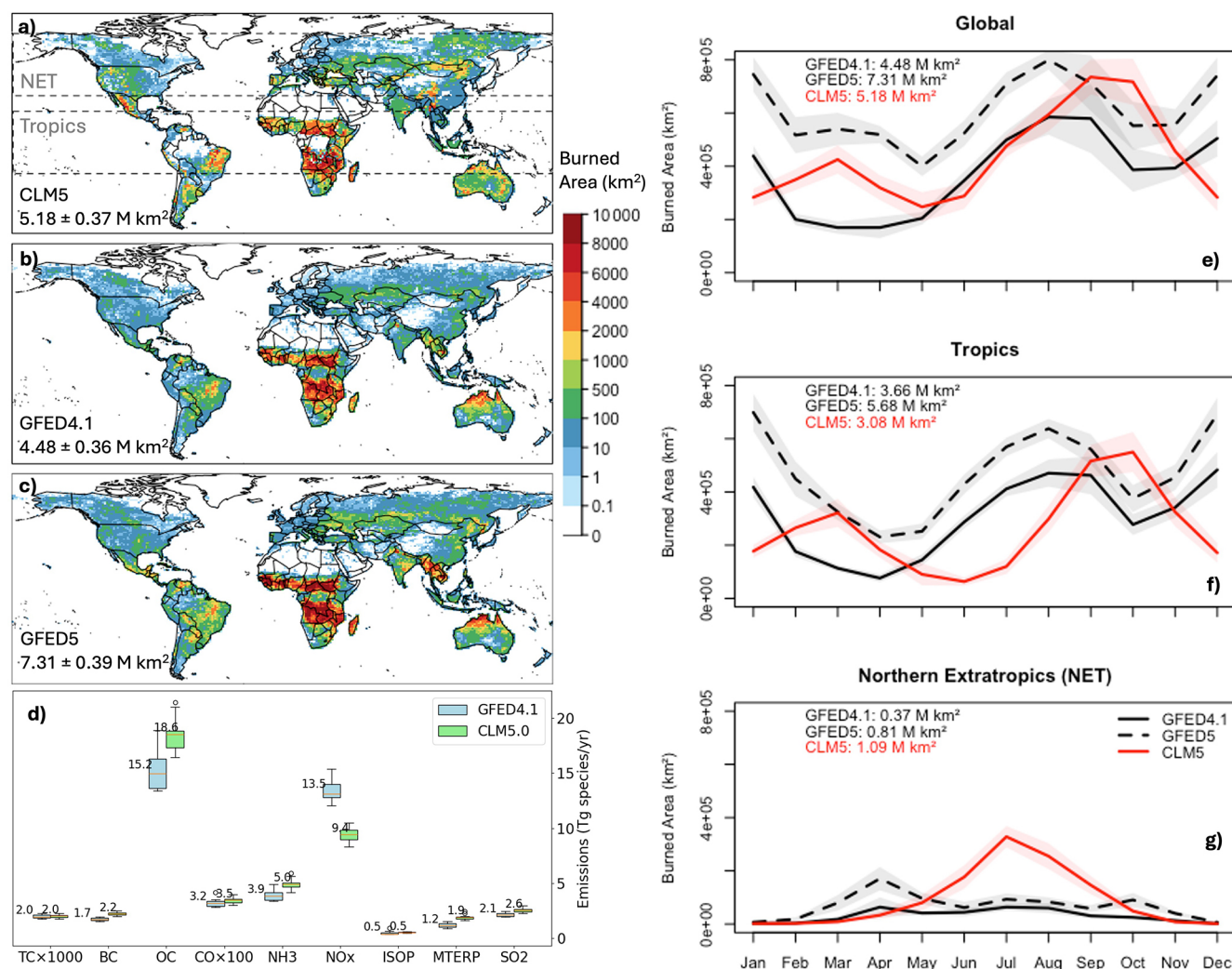


**Figure 1.** Comparison of CLM5-simulated results (2015–2024, SSP1) with the Global Fire Emissions Database (2007–2016 for GFED4.1; 2011–2020 for GFED5). Spatial distribution of burned area for (a) CLM5, (b) GFED4.1, and (c) GFED5 are averaged for a decade. (d) Global annual emissions of main fire-emitted species, including total carbon (TC), black carbon (BC), organic carbon (OC), carbon monoxide (CO), ammonia (NH<sub>3</sub>), nitrogen oxide (NO<sub>x</sub>), isoprene (ISOP), monoterpene (MTERP), and sulfur dioxide (SO<sub>2</sub>) are compared between CLM5 and GFED4.1 for the same time period as that of burned area. Monthly climatology of BA for (e) global, (f) tropical (20° S–20° N), and (g) northern extratropics (NET: 30–70° N) regions are compared for CLM5 with GFED4.1 and GFED5. Shaded areas represent interannual variability (±SD).

the last ten years. Our results also align with satellite-based estimates for 2001–2018, which report an average global BA of 4.63 million km<sup>2</sup> and a range of 3.9 to 5.2 million km<sup>2</sup> (Lizundia-Loiola et al., 2020). Despite some biases, the model performance is robust, with a normalized mean bias of +15.6 % (−29.1 %) and a correlation coefficient ( $R$ ) of 0.64 (0.62) when compared to GFED4.1 (GFED5). The underestimation relative to GFED5 likely arises from CLM coarse resolution, fixed land-use configuration, and limited representation of small fires (Hantson et al., 2020; Chen et al., 2023a).

To further assess the ability of CLM5 to capture temporal fire dynamics, we compared monthly BA across global,

tropical (20° S–20° N), and northern extratropical (NET: 30–70° N) regions (Fig. 1e–g). CLM5 reproduces the observed double-peak seasonal cycle in the tropics, which is also reflected in the global mean due to the dominance of tropical fire activity. This pattern, visible in both GFED4.1 and GFED5, likely reflects distinct early and late dry season burning phases, though with some discrepancies in the timing and magnitudes of the peaks, likely due to known precipitation biases or underrepresentation of early dry season fires and differences in the fuel build-up season (Hantson et al., 2020; Li et al., 2024). In NET regions, CLM5 overestimates BA (1.09 million km<sup>2</sup> vs. 0.37 and 0.81 million km<sup>2</sup> in GFED4.1 and GFED5, respectively), particularly during



summer months, potentially due to over-sensitivity to fire weather or fuel availability. Despite these regional biases, CLM5 broadly reproduces key spatiotemporal patterns of global fire regimes. While CLM5 retains the core structure of CLM4.5, key updates to fuel moisture sensitivity and agricultural fire treatment improve fire sensitivity (Lawrence et al., 2019). Comparison of CLM performance with other fire models within the Fire Model Intercomparison Project (FireMIP) also reported that CLM reasonably reproduces the spatiotemporal variability in global fires (Li et al., 2019; Hantson et al., 2020). Importantly, Hantson et al. (2020) reported CLM as the only model to reproduce the double-peak fire season, while all other models produce a single summer peak, indicating its improved ability to simulate fire dynamics. Recent studies have further compared different Earth system models and found CESM estimates closer to observations (e.g., Li et al., 2024).

Emissions of key fire-related species such as total carbon (TC), black carbon (BC), organic carbon (OC), and nitrogen oxides ( $\text{NO}_x$ ) were also compared against GFED4.1, as data are not available for GFED5 (Fig. 1d). Decadal averaged results show strong agreement for most species, with TC emission of  $2017 \pm 158 \text{ Tg yr}^{-1}$ , closely approximating the GFED4.1 estimates of  $1997 \pm 175 \text{ Tg yr}^{-1}$ . However, certain species, such as OC, are slightly overestimated, while  $\text{NO}_x$  emissions are marginally underestimated.

### 3.2 Trends and spatial variations in burned area and carbon emissions

The projected impact of climate change on BA and carbon emissions shows a marked increase under low and high warming scenarios. Global BA is projected to increase by  $+6383 \text{ km}^2 \text{ yr}^{-1}$  under SSP1 and  $+7465 \text{ km}^2 \text{ yr}^{-1}$  under SSP3 between 2015 to 2100 (Fig. 2a), resulting in an overall increase of  $+0.73$  and  $+0.68$  million  $\text{km}^2$ , respectively, by the 2090s compared to the present day. These increases are particularly centered toward the NET (Fig. S2). BA reductions of  $\sim 25\%$  in the tropics in high warming scenario negate BA increases in high northern latitudes, leading to a lower global average under SSP3 as compared to SSP1, which sees sharp increases in tropics (Fig. 2b–d). However, the overall rate of increases in BA under SSP3 is approximately  $+1000 \text{ km}^2 \text{ yr}^{-1}$  higher relative to SSP1, primarily driven by sharp increases in fuel supply, reduced soil moisture, and favorable meteorology, such as elevated surface temperature and reductions in RH (Fig. S3; see Sect. 3.2).

We found important differences at a regional scale. In NETs, particularly near  $60^\circ \text{N}$ , where boreal forests dominate alongside alpine forests and shrublands, BA and TC emissions are projected to increase by over  $150\%$  in both SSP scenarios (Figs. 3a–d and S4). This intensification is most evident in boreal region, where the trend in BA reaches  $+5237 \text{ km}^2 \text{ yr}^{-1}$  under SSP1 and  $+8515 \text{ km}^2 \text{ yr}^{-1}$  under SSP3. In contrast to the pronounced increases in boreal BA,

our simulations project localized decreases in BA across parts of the humid tropics as well as temperate regions such as the UK and eastern US. In tropical rainforest regions, elevated precipitation and humidity under future climate scenarios likely suppress fire activity by maintaining higher fuel moisture levels and shortening the fire season. In temperate zones such as the UK and eastern US, projected climate changes (e.g., increased rainfall or limited warming) may reduce conditions that promote fires. These declines occur despite fixed land use and populations, indicating that purely climatic effects can suppress fire activity in certain fuel-rich or moisture-sensitive systems. Additionally, tropical regions show slight decline in BA under SSP3 ( $-2429 \text{ km}^2 \text{ yr}^{-1}$ ) and SSP1 ( $-64 \text{ km}^2 \text{ yr}^{-1}$ ), both remaining statistically insignificant at  $95\%$  level (Fig. 3e–h). Despite the upward trends in NET fires, the tropics remain the dominant contributor to total global BA and carbon emissions during the 21st century, underscoring a shifting geographic balance of wildfire risks.

Differences in carbon emissions closely align with the pattern of BA (Figs. 3, S5). Boreal regions emerge as the primary contributors to the overall increase in TC emissions, where it increases at the rate of  $4.36$  and  $6.72 \text{ Tg yr}^{-1}$  under SSP1 and SSP3 scenarios, respectively. In contrast, the tropical region experiences a marginal difference in TC emissions in both scenarios. Similar trends are observed for other carbonaceous species, including BC, OC, and carbon monoxide (CO), thus, TC is emphasized in the main text as a representative carbonaceous species. By 2090s, fire-related carbon emissions are expected to rise by  $22\%$ – $32\%$  compared to the present-day levels. Notably, emissions from regions above  $50^\circ \text{N}$  are projected to surge by more than two folds, underscoring the substantial influence of high-latitude fires in shaping future global carbon budgets. In addition, the carbon emitted from boreal fires may become as important as tropical fires, in terms of magnitude ( $\sim 1000 \text{ Tg C yr}^{-1}$ ) by the end of the century in a high warming world.

Figure 4 highlights a significant shift in global fire regimes and their carbon emissions across SSP1 and SSP3 scenarios. Under both scenarios, global BA shows a slight increase during 2050s and 2090s compared to the baseline (2020s), but regional trends differ markedly. While tropical BA remains nearly stable or declines slightly, boreal BA increases significantly in both cases, rising from  $1.09$  million  $\text{km}^2 \text{ yr}^{-1}$  during baseline to  $1.50$  million  $\text{km}^2 \text{ yr}^{-1}$  under SSP1 and  $1.70$  million  $\text{km}^2 \text{ yr}^{-1}$  under SSP3. Consequently, the boreal-to-tropics BA ratio increases from  $0.35$  at baseline to  $0.46$  under SSP1 and  $0.57$  under SSP3, indicating the growing contribution of boreal fires relative to the tropics. Similarly, TC emissions exhibit a marked redistribution, with global emissions increasing from  $2017 \text{ Tg yr}^{-1}$  at baseline to  $2535 \text{ Tg yr}^{-1}$  under SSP1 and  $2552 \text{ Tg yr}^{-1}$  under SSP3. While tropical carbon emissions decline slightly, boreal emissions surge from  $547 \text{ Tg yr}^{-1}$  at baseline to  $894 \text{ Tg yr}^{-1}$  under SSP1 and  $1032 \text{ Tg yr}^{-1}$  under SSP3. This shift is also evident in the boreal-to-tropic TC emission ratio, which in-

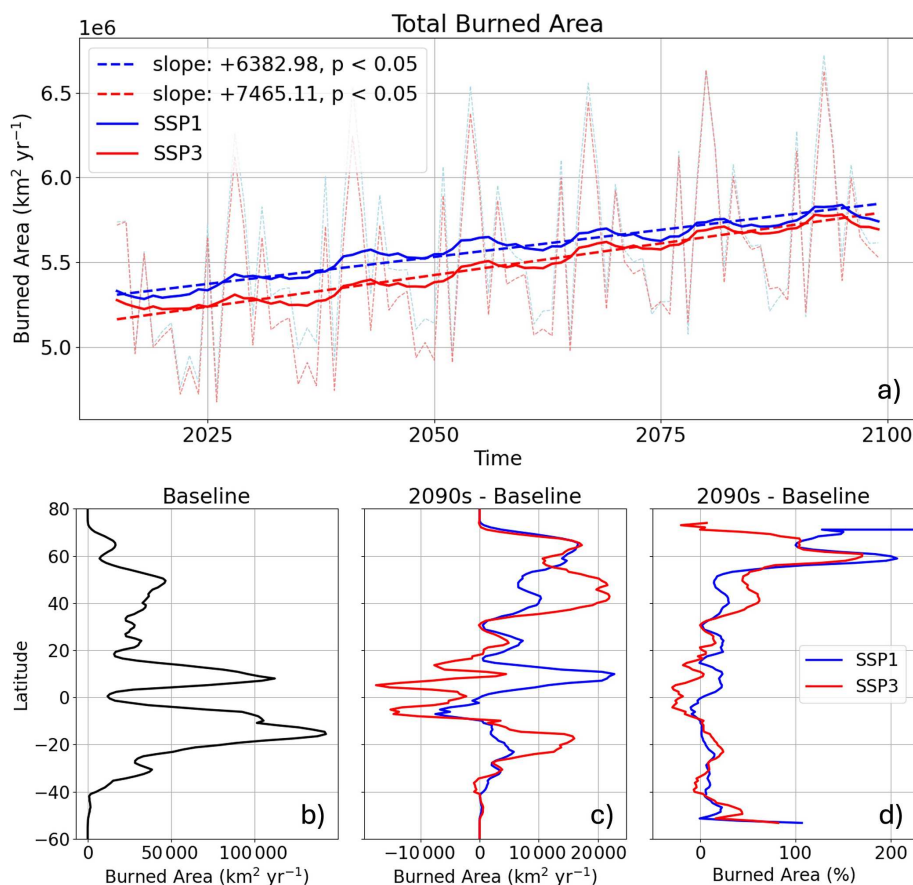


**Figure 2.** Trend analysis of global burned area (BA) during the 21st century (2015–2100) under SSP1 and SSP3 climate scenarios. In panel a), dotted lines indicate the annual variations and their trends, while the solid lines indicate the 30-year centered moving average. The latitudinal variations of BA during (b) baseline (averaged 2015–2024; SSP1) and its (c) absolute and (d) percentage future differences are shown at 5° moving average.

creases from 0.50 at baseline to 0.76 under SSP1 and 0.97 under SSP3, as well as the boreal-to-global ratio, rising from 27 % to 35 % under SSP1 and 40 % under SSP3. These trends underscore the growing dominance of boreal fires in driving global carbon emissions under future climate scenarios, with more pronounced increases under SSP3. The results highlight the critical role of boreal fire regimes in amplifying climate feedbacks and the need for region-specific fire management strategies to mitigate their disproportionate impact on the global carbon cycle. The interrelationships among BA, carbon emissions, and meteorological factors are further discussed in subsequent sections.

### 3.3 Key drivers of burned area in future climates

To identify the main factors influencing climate-driven wildfires, we analyzed the spatial variations (Fig. S3) and correlations between BA and meteorological factors, vegetation dynamics, and carbon emissions. To isolate interannual variability and minimize the influence of long-term trends, we performed a Pearson correlation coefficient analysis on de-

trended annual mean data for each grid cell from 2015 to 2100. We found strong correlations of BA with meteorological variables, total vegetation carbon (TOTVEGC), and TC emissions for both SSP1 (Fig. 5) and SSP3 (Fig. S6) scenarios. BA is positively correlated with surface temperature across most fire-prone regions ( $R > 0.6$ ), consistent with the role of warming in enhancing fuel flammability and increasing fire risks (e.g., Abatzoglou and Williams, 2016; Wu et al., 2021). A strong positive correlation also appears between BA and total vegetation carbon in Eurasian (Steppe) and tropical grasslands (e.g., African savanna, parts of Australia), where warmer and wetter conditions stimulate plant productivity, thereby increasing the fuel supply and fire risks. This is also likely amplified under future elevated  $\text{CO}_2$ , which enhances photosynthesis and fuel accumulation via fertilization effects (Lawrence et al., 2019; Walker et al., 2021; Allen et al., 2024). Meanwhile, in forested regions, the correlation between BA and vegetation carbon is often negative, suggesting that dense woody vegetation may suppress fire through improvement in plant water use efficiency, thereby retaining soil moisture and lowering fuel flammability. These findings sup-



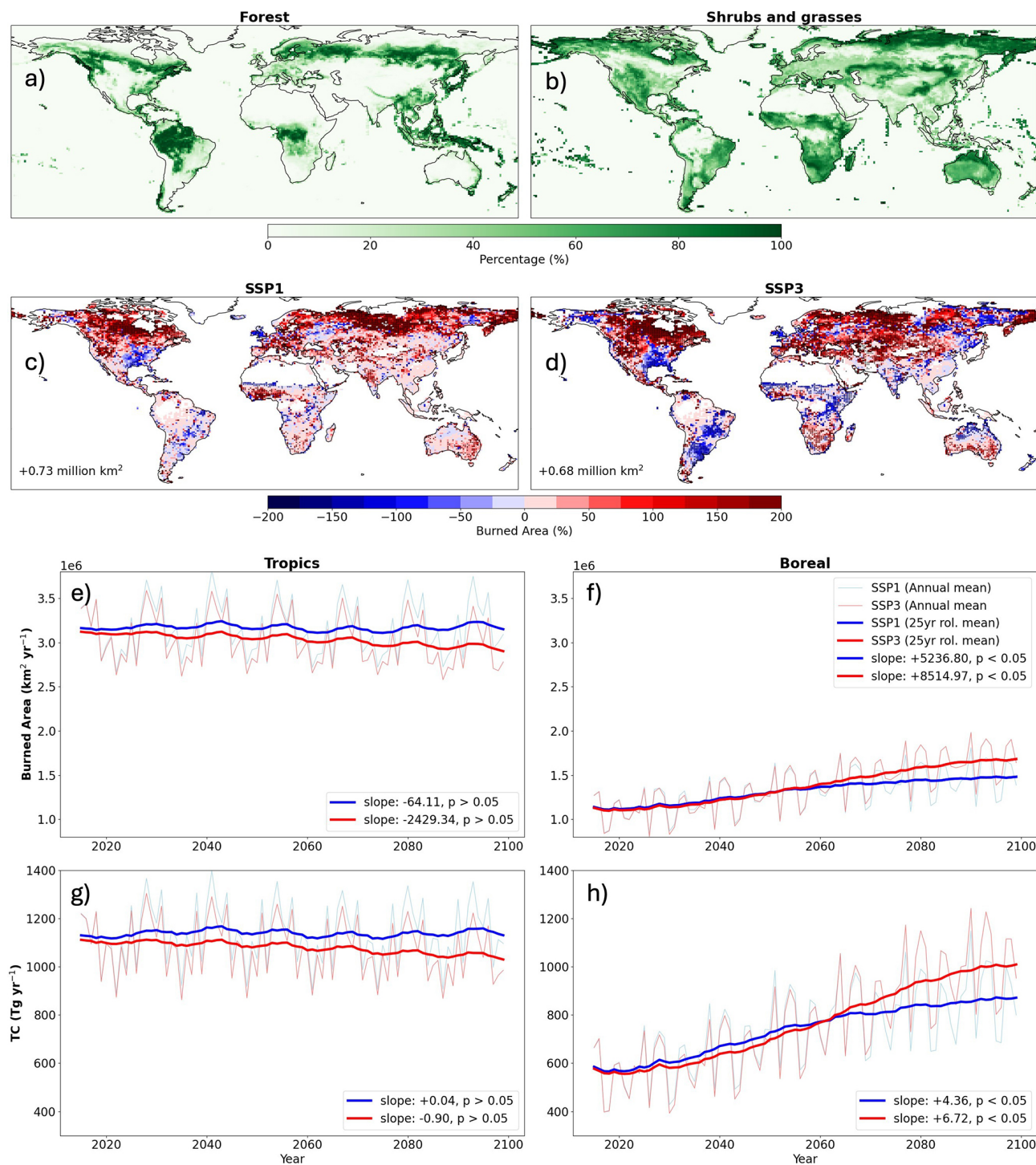


**Figure 3.** Spatial variations of present-day land cover: (a) forest and (b) shrubs and grasses, derived from the product of natural plant functional types (PCT\_NAT\_PFT) and natural vegetation (PCT\_NATVEG) fractions, summed over the relevant natural PFTs (forest: 1–8, shrubs and grasses: 9–15). Percentage difference in BA [future (2090 to 2099) – baseline (2015 to 2024)] under (c) SSP1 and (d) SSP3 scenarios. Trend lines for (e, f) BA and (g, h) TC emissions are shown for tropics and northern extratropics (NET) regions throughout the 21st century. Dots in panels c and d indicate regions with significant difference at 95 % confidence interval. Lighter colors of trend lines represent annual variations, while bold lines indicate a 30-year moving average.

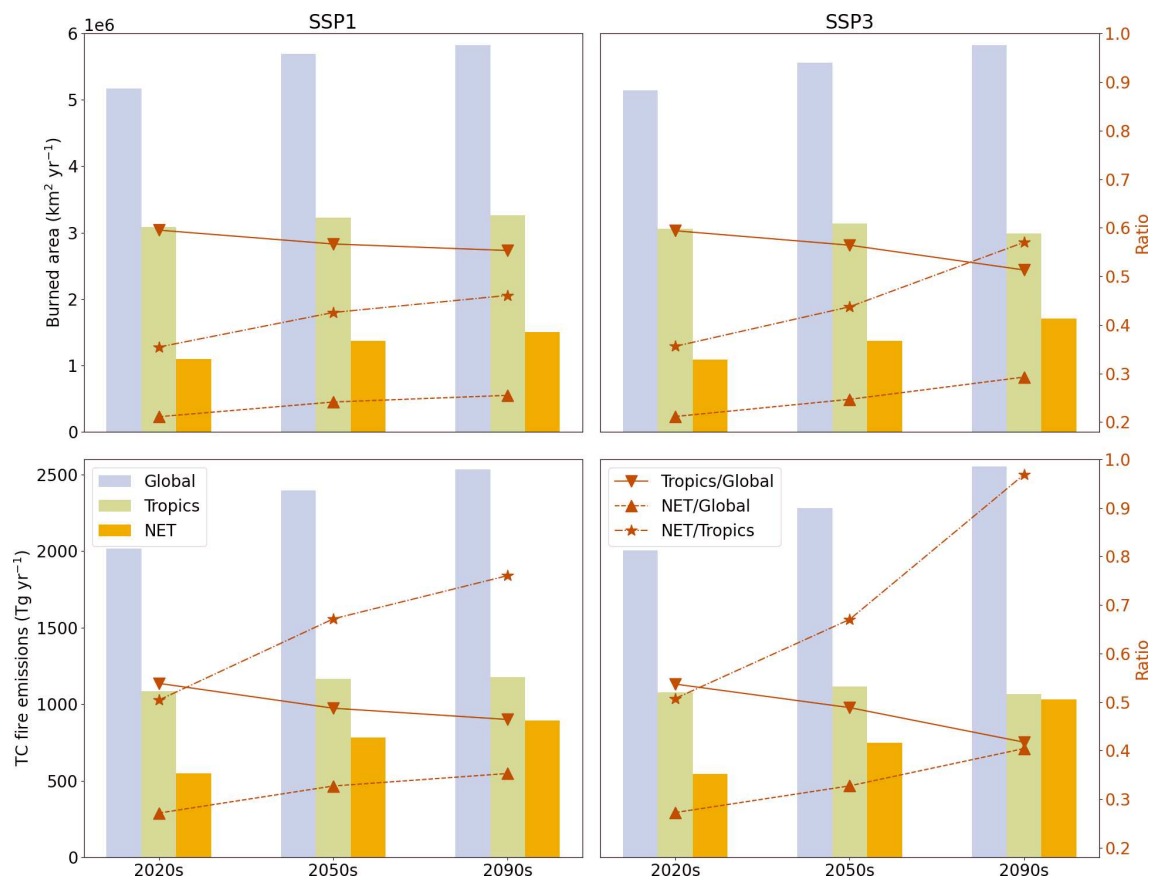


**Figure 4.** Present day (2020s: 2015–2024) and future (2050s: 2050–2059; 2090s: 2090–2099) decadal mean of burned area (BA) and total carbon (TC) emissions across global, tropics ( $20^\circ \text{S}$ – $20^\circ \text{N}$ ), and northern extratropics (NET:  $30^\circ$ – $70^\circ \text{N}$ ) regions (bar-plot) under low (SSP1) and high (SSP3) warming scenarios. The ratio of BA and TC emissions against tropics / global, NET / global, and NET / tropics is presented as line plots, which show the increasing contribution of NET region on BA and TC emissions.

port the notion that herbaceous fuels respond more rapidly to fire-conductive weather, while forests may buffer such effects due to slower drying and deeper rooting (Jones et al., 2022). Effects of these individual forcing factors, such as climate,  $\text{CO}_2$ , and land use, on fuel availability and combustibility have also been previously discussed for historical fires using several climate models under FireMIP (Li et al., 2019).

BA shows widespread negative correlations with moisture-related variables (e.g., RH, 10 cm soil moisture, precipitation, and CWA), consistent with their role in suppressing fire through increased fuel moisture and reduced flammability (Jolly et al., 2015). Soil moisture, in particular, has a key indirect control on wildfire activity, influencing both vegetation stress and fuel moisture content. Although the model does not simulate dead fuel moisture explicitly, soil moisture serves as a proxy for fuel combustibility. Drier soil conditions reduce live fuel moisture and increase the likelihood of ignition and fire spread. However, persistently dry conditions may also suppress vegetation growth and thus reduce fuel availability, which can lead to lower fire activity in some cases (Turco et al., 2017).

In tropical forests, high precipitation and soil moisture continue to reduce BA, consistent with fuel combustibility suppression. However, in semiarid savannas, modest precipitation enhancements promote grass growth, boosting fire-prone fine fuel loads. However, upper soil moisture (10 cm) may not fully represent deeper root zones in forests and can vary in flammability (Markewitz et al., 2010; Lawrence et al., 2019). These contrasting relationships demonstrate region-specific climate-fire dynamics, mediated by vegetation types and fuel responses to water availability.

Wind speed shows mixed correlations with BA. In fire-prone regions such as Australia and parts of South America, positive correlations indicate that stronger winds enhance fire spread. In contrast, in some high-latitude northern regions, increased wind is possibly associated with the influx of cooler, moister air masses, leading to a suppression of fire activity.

BA shows a strong spatial correlation with TC emissions ( $R > 0.80$ ) across most regions, highlighting the model-inherent link between area burned and carbon output. Further analysis of the differences in carbonaceous species also

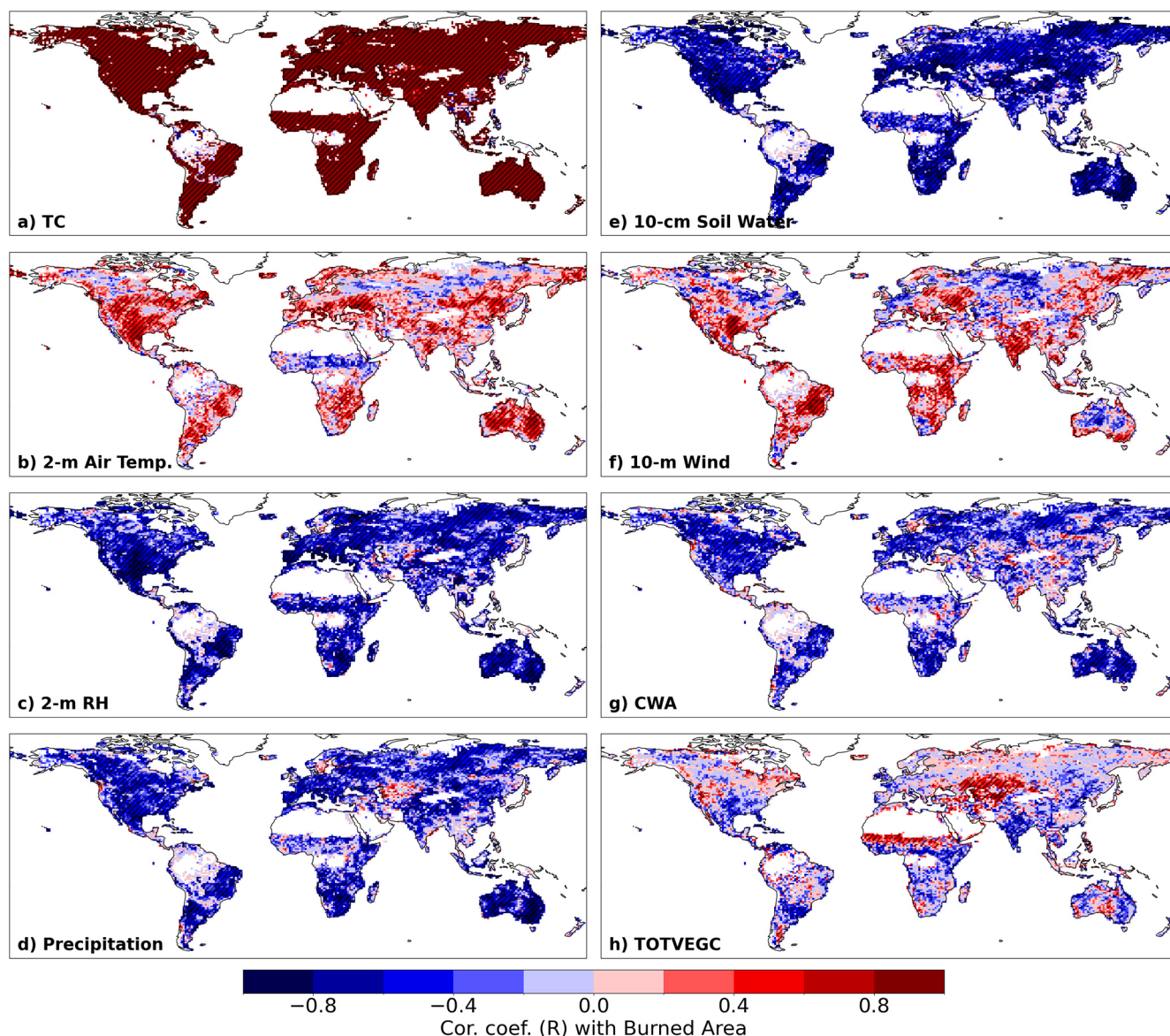


**Figure 5.** Pearson correlation ( $R$ ) on annual mean time series data (2015 to 2100) between detrended burned area (BA) and (a) TC, (b–g) meteorological variables (2 m surface temperature, 2 m relative humidity (RH), precipitation, 10 cm soil water, 10 m wind velocity, and climate water availability (CWA = precipitation – evapotranspiration)), and (h) total vegetation carbon (TOTVEGC) under SSP1 scenario. Hatch lines are shown over regions with a 95 % significance level.

corroborates the robust correlation with differences in BA ( $0.56 < R < 0.71$ ,  $p < 0.05$ ; Fig. S7), underscoring the synergistic effect of BA on carbon emissions. Although increased BA generally leads to higher emissions, a reduction in grassland BA accompanied by forest fire increases may result in higher emissions despite declining total BA (Zheng et al., 2021).

### 3.4 Seasonality of wildfires

Distinct seasonal variations in BA and wildfire emissions are observed for both present-day conditions and future climate

forcings (Figs. 6, S8). The most substantial increase in BA and carbon emissions occur during the boreal summer (June to August), particularly in the Northern Hemisphere, including regions such as the western United States, Canada, and Russia (Fig. S9). In the Southern Hemisphere, BA increases are predominant during its warmer periods (September to February), most notably in southern Africa and Australia. Conversely, tropical regions experience a sharp decline in BA primarily from December to March under SSP3, while SSP1 shows an increase during the same period, highlighting the varied regional response to climate change. Among these seasonal variations, NET regions exhibit a pronounced rise



in both BA and carbon emissions during the summer months, and the fire season may potentially be extended by an additional month by 2100 in temperate latitudes (30–50° N) under high-warming conditions (SSP3).

To further investigate the drivers behind the sharp rise in BA and carbon emissions in boreal regions, we conducted a detailed analysis focusing on both summer (Fig. 7) and winter seasons (Fig. S10). Our results show a pronounced seasonal contrast, with the largest BA increases occurring during the boreal summer months. During this period, several climatic factors converge to create optimal wildfire conditions: higher temperatures, increased vegetation productivity, reduced RH, and lower soil moisture. These factors, especially in boreal forests, amplify fire outbreak risks. Increased vegetation, while potentially serving as a carbon sink, may contribute to higher fire risks by increasing fuel availability, especially under warmer and drier conditions (Flannigan et al., 2009).

Both SSP1 and SSP3 scenarios predict a significant rise in boreal wildfires, with the increase notably more severe under SSP3, where heightened temperatures result in steeper declines in RH and CWA. Elevated temperatures exacerbate evapotranspiration, leading to drier vegetation and surface conditions that further amplify fire risks. In contrast, the winter season exhibits minimal differences in BA, despite rising temperatures and reduced RH. Extreme winter cold effectively suppresses wildfire ignition, regardless of potential climatic shifts. Elevated soil moisture and CWA during winter, combined with frozen ground and snow cover, limit fire activity, as projected warming remains insufficient to reach the threshold required to sustain fire during winter.

Spatial analysis reveals that the most significant increases in BA and fire emissions occur in boreal Eurasia, where temperature anomalies are especially pronounced. This region shows large areas of intensified fire activity, with isolated pockets of reduced BA under SSP3, possibly due to increased winter precipitation or soil moisture that offsets fire risk.

Feature importance results from CLM5 consistently identify 10 cm soil water content (influencing fuel availability and dryness), RH, and vegetation carbon (influencing canopy and surface fuel loads) as primary predictors of wildfire activity (Fig. 8). These three factors alone explain over 55 % of model variance. While CLM5 does not explicitly simulate dead fuel moisture, lower soil moisture is often associated with drier fuels, increasing fire susceptibility.

Comparison with GFED5 observations reveals fundamental challenges in comparing fire drivers across different spatial domains and data sources. The driver importance itself varies dramatically within GFED5 – precipitation dominates globally (23.6 %) but ranks fifth in high latitude regions (13.0 %), CWA and windspeed gain importance at high latitudes (Fig. S11). While CLM5 shows strong high latitude fire predictability ( $R^2 = 0.70$ ), GFED5 low predictive skill ( $R^2 = 0.23$ ) indicates environmental variables alone poorly explain observational high latitude fires, mainly due

to zero-inflation noted in Sect. 2.4. Despite this, both CLM5 and GFED5 consistently identify moisture variables as top drivers, validating CLM5 representation of water limitation as a key boreal fire constraint after biofuel availability.

SHAP analysis further reveals the nonlinear and context-dependent behavior of environmental drivers. Low soil moisture and high vegetation carbon values substantially increase predicted BA, underscoring the critical role of dry and abundant fuels. Surface temperature and RH show moderate yet consistent effects: higher temperatures and lower RH are associated with elevated fire risks. In contrast, precipitation and wind speed exhibit weaker and more variable influences, often depending on local fuel conditions. Moreover, high CWA contributes to elevated BA as it may facilitate vegetation growth and thus indirectly accumulate fuel required for fires, reflecting fuel accumulation during wetter conditions followed by subsequent drying. These insights emphasize both the dominant controls and complex interdependencies shaping wildfire risks in boreal regions. Although these ML results provide useful diagnostic insights into feature importance, they are inherently limited by the underlying correlations in the input variables and model structure. Future work should explore process-level attribution through sensitivity simulations using fixed climate forcings within CLM5.

This analysis underscores the need for a deeper understanding of the interplay between climatic drivers, vegetation dynamics, and fire behaviors to mitigate boreal wildfire risks under future climate scenarios. While machine learning models identify soil water content and vegetation carbon as the most critical predictors of wildfire activity, rising surface temperatures play an indirect yet pivotal role. Elevated temperatures exacerbate evapotranspiration, reduce RH, and lower soil moisture, thereby intensifying fire risk. These cascading effects highlight the importance of considering temperature as a key enabling factor that interacts with vegetation and hydrological conditions to drive wildfire dynamics. Additionally, the positive correlation between BA and vegetation carbon suggests that future fire management strategies should consider shifts in vegetation growth patterns driven by changing climatic conditions, particularly in boreal ecosystems where temperature and water availability are limiting factors. CLM5 tracks multiple vegetation carbon pools, including fine roots and dead biomass (Lawrence et al., 2019). However, the fire module uses an aggregated fuel load for ignition and spread, without differentiating the structure of fine and dead fuels, which may overemphasize the influence of total biomass in controlling fire behavior.

Under low and high warming climates, the projected sharp rise in boreal wildfires emphasizes the necessity of comprehensive fire management strategies that address the complex links between climate and vegetation, as well as the seasonality of these interactions. The expected increase in high-latitude fire activity and associated carbon emissions will significantly contribute to the global carbon budget. Targeted mitigation efforts, such as prescribed burns or enhanced fire

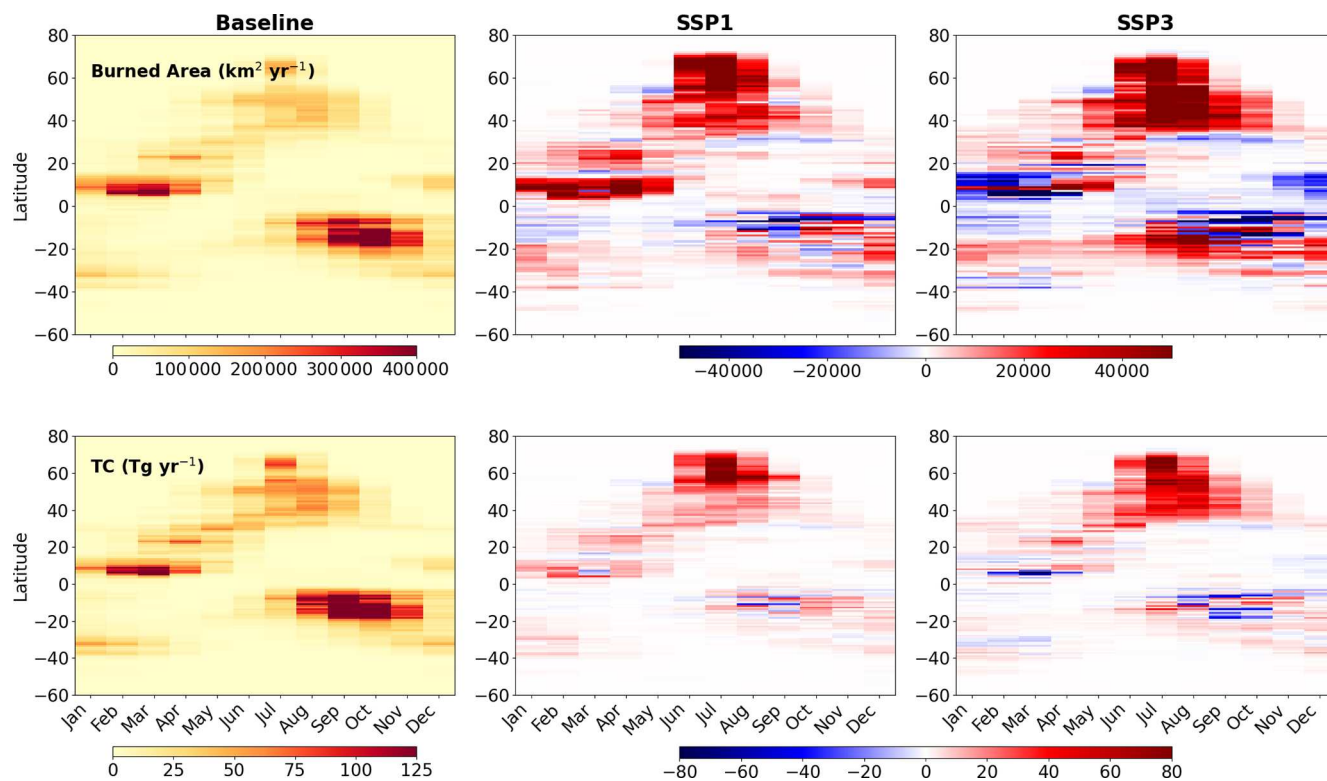


**Figure 6.** Latitudinal monthly variations in burned area and total carbon emissions at baseline (2015–2024 average) and their future (2090–2099 average) differences in SSP1 and SSP3.

suppression during critical periods, will be crucial. Furthermore, the cascading impacts of wildfires on carbon cycling and atmospheric composition – including increased emissions of BC and OC – highlight the urgency of adaptive strategies. These strategies must account for the feedbacks between climate change, vegetation growth, and fire behaviors to effectively manage future wildfire risks.

#### 4 Discussion

This study highlights a significant shift in wildfire dynamics, particularly in NET regions under future climate scenarios, using a state-of-the-art fire-enabled global terrestrial system model that explicitly simulates interactive fire with active biogeochemistry. Our findings indicate that boreal regions, especially around 60°N, could experience a staggering increase in BA by up to 200 % under high-warming scenarios (SSP3-7.0), primarily driven by reduced soil moisture and increased vegetation carbon, creating dryer and more combustible conditions. These results align with previous studies predicting an intensification of Arctic fires due to climate-induced extreme fire weather, increased lightning activity, and drier fuel conditions (McCarty et al., 2021). Furthermore, Abatzoglou et al. (2019) explored that regions experiencing heightened fire weather could double at 3°C warming

compared to 2 °C above preindustrial levels, emphasizing the significant influence of anthropogenic climate change (Turco et al., 2023).

While warming and drying conditions dominate fire risk trends, elevated atmospheric CO<sub>2</sub> plays an important complementary role by increasing vegetation carbon and influencing plant water dynamics. In CLM5, CO<sub>2</sub> fertilization enhances photosynthesis and plant growth, contributing to greater fuel loads in fire-prone biomes, particularly at high latitudes. CO<sub>2</sub> also improves water-use efficiency, which can buffer soil moisture loss under warming. Although our simulations apply changing CO<sub>2</sub> and climate simultaneously, making it difficult to isolate their respective effects, their combined impact is evident in regions where biomass accumulation and fuel dryness jointly elevate BA and emissions. This highlights the importance of considering both physiological and climatic fire drivers in future scenario planning.

Our results also emphasize the role of other meteorological variables in modulating fire activity. While rising temperatures and CO<sub>2</sub>-driven vegetation growth contribute to heightened fire risks, wind speed and precipitation exert secondary influences. Stronger wind speed at high latitudes can suppress fire spread by transporting colder, moist air, whereas increased precipitation can paradoxically increase fire risk by stimulating vegetation growth in water-stressed areas, thereby increasing fuel loads. These results are con-

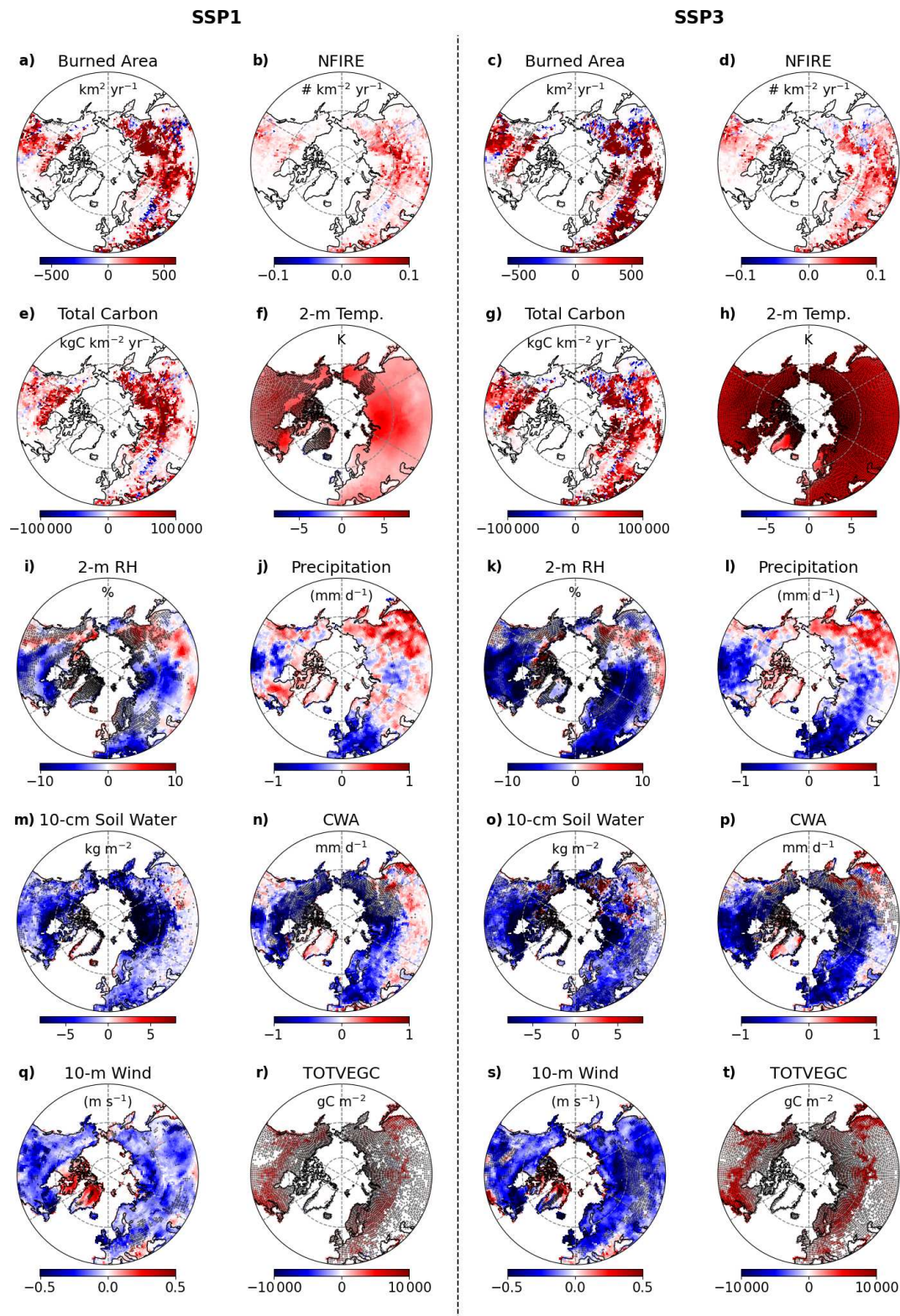


**Figure 7.** The 2090s fire season (JJA) anomaly (relative to the present day) for modeled burned area, number of fires (NFIRE), TC emissions, meteorology, and total vegetation carbon (TOTVEGC) in the boreal region ( $\geq 40^\circ \text{N}$ ) for SSP1 and SSP3. Dots indicate regions with a 95 % significance level.



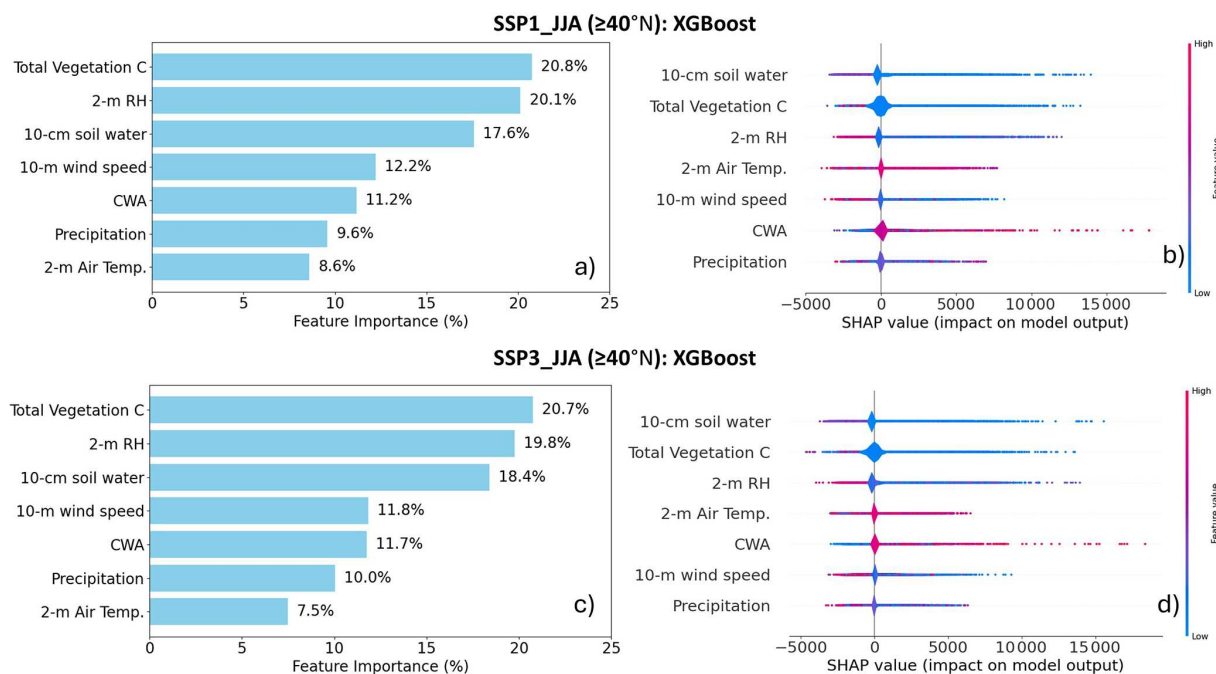


**Figure 8.** Feature importance and SHAP summary plots showing analysis of environmental drivers of wildfire activity during boreal summer (JJA) over northern latitudes ( $\geq 40^\circ\text{N}$ ) using XGBoost machine learning model under (a, b) SSP1 and (c, d) SSP3 scenarios.

sistent with historical wildfire studies (Zheng et al., 2023), which documented that warmer and drier conditions in boreal forests contributed to the rapid wildfire expansion from 2000 to 2020. Our findings further extend these insights into the future, demonstrating how climate and vegetation changes will continue shaping wildfire trends.

The projected intensifications of NET fires has significant ecological and climatic implications. Increased fires in subalpine regions reduce species diversity, leading to greater forest homogeneity and disrupting entire ecosystems (Cassell et al., 2019; Halofsky et al., 2020). The transition of boreal forests from carbon sinks to net carbon sources due to increased fire emissions could further amplify warming trends through enhanced greenhouse gas concentrations and BC deposition on Arctic ice, accelerating ice melt (e.g., Liu et al., 2014; McCarty et al., 2021; Virkkala et al., 2025). Furthermore, the degradation of boreal ecosystems threatens biodiversity, disrupts regional hydrological cycles, and deteriorates air quality due to increases in particulate and ozone precursors. These findings underscore the necessity for integrating wildfire dynamics into climate policy frameworks to effectively mitigate future risks.

While NET wildfires exhibit a strong upward trend, tropical regions exhibit a contrasting response, with either stable or decreasing trend in BA under future climate scenarios. This pattern is consistent with previous studies (Veira et al., 2016; Jones et al., 2022), which reported increasing BA at higher latitudes but declines in the tropics. Climate driven alternations in temperature and precipitation patterns introduce

uncertainties in fire regimes across different biomes, highlighting the complexity of climate-fire interactions (IPCC, 2014; Fasullo et al., 2018).

Seasonal variations further illustrate the complexity of factors governing wildfire dynamics. Despite rising temperatures in boreal summer and winter, the sharp rise in BA and carbon emissions in the NET region is confined to summer, as winter wildfires are suppressed by persistent cold temperatures and snow cover. Additionally, in temperate regions ( $30\text{--}50^\circ\text{N}$ ), high warming scenario extended the fire season, leading to longer fire durations (Senande-Rivera et al., 2022). Moreover, in the recent two decades, the extreme wildfire events have increased by twofold, particularly in boreal and temperate conifer regions (Cunningham et al., 2024). These findings emphasize the need for seasonally and regionally tailored fire management strategies. In temperate, populated regions, targeted interventions such as controlled burns, thinning or fuel reductions, and soil moisture enhancement can mitigate wildfire risks. However, in sparsely populated NET regions, where large-scale fires occur in remote landscapes with limited accessibility, direct intervention is often challenging due to larger fire size and lower government priority. Thus, integrating wildfire risks into climate impact assessments, carbon sequestration estimates, and long-term climate feedback analysis is crucial for understanding the broader implications of NET wildfires. Predictive models incorporating wind speed, precipitation patterns, and fuel accumulation dynamics can further aid in resource allocation and preparedness efforts. A nuanced approach that considers both

management feasibility and the role of NET fires in global climate systems will be essential for mitigating their impacts on air quality, biodiversity, and human health under future climate scenarios.

Several limitations of this study warrant further investigation and consideration when interpreting our results:

- Attribution experiments: Our study isolates the climate effect by holding anthropogenic influence (changes in land use and population density) constant. While this provides a controlled framework for evaluating climate-driven wildfire risks, real-world fire dynamics are shaped by a broader set of factors. Future land use changes – such as agricultural expansion, forest fragmentation, or abandonment – can alter fuel continuity and flammability. For instance, fragmentation may reduce fire spread by breaking fuel connectivity, while deforestation or abandonment could increase fire risk by creating more open, combustible landscapes. Similarly, population growth and urbanization may lead to more frequent human ignitions or enhanced suppression capacity, depending on regional context. These socioeconomic dynamics, which have already contributed to declining BA in recent decades (e.g., Andela et al., 2017; Forkel et al., 2019), are not captured in our simulations. In addition, our interpretation of fire-climate relationships is based on statistical methods, which are inherently correlative. Future research would benefit from targeted sensitivity simulations that systematically vary climate drivers (e.g., CO<sub>2</sub>, temperature, precipitation) or land use parameters, either independently or in combination. Such factorial experiments would enable more rigorous causal attribution and improve confidence in regional fire projections under complex future scenarios.
- Regional differences: Relative importance of climate versus human activity is expected to differ across regions. Boreal ecosystems are primarily sensitive to climatic factors such as fuel availability, soil moisture, and fire weather conditions, whereas tropical regions are more strongly influenced by human land use change, agricultural expansion, and fire suppression practices (e.g., Andela et al., 2017; Forkel et al., 2019; Wu et al., 2021). This regional heterogeneity highlights the need for caution when interpreting climate-only fire projections, particularly in human-dominated landscapes. Notably, our findings show that the largest projected increase in BA and carbon emissions occur in boreal regions, where human activity is comparatively limited. This reinforces the robustness of our climate-driven projections in these areas. Conversely, the simulated declines in tropical burned area despite constant socioeconomic forcings suggest that climate-induced changes, such as increased precipitation, may independently drive fire suppression in some regions. These contrasting patterns underscore the critical role of regional context in interpreting future wildfire trends.
- Model resolution and representation: The CLM5 model, with its relatively coarse spatial resolution (~ 100 km), may lead to underrepresentation of short-term and small-scale fires, particularly those driven by local ignition sources, land use changes, or fine-scale vegetation patterns. These fires, although individually small, can have cumulative ecological and atmospheric impacts, especially in fragmented landscapes or human-dominated regions. Additionally, our analysis relies on 10 cm topsoil moisture as a proxy for assessing fuel dryness, which may not fully reflect water availability for deep-rooted vegetation in forest ecosystems. However, CLM5 fire module internally relies on root-zone soil wetness to estimate fuel combustibility, which captures moisture availability over a deeper soil profile. This distinction introduces some approximation in our interpretation, especially in ecosystems where deeper soil layers better reflect vegetation water access and fire susceptibility.
- Ignition sources and feedback effect: Natural ignitions are prescribed based on NASA lightning frequency data averaged from 1995 to 2011, limiting the scope of future variability. Future studies should integrate interactive lightning simulations that evolve with changing climate conditions. Improved representations of fire behavior, vegetation dynamics, two-way feedback mechanisms, and socioeconomic drivers will be essential to comprehensively understand wildfire risks in a changing climate. Coupling fire models to atmospheric models can also enhance our understanding of how wildfires influence regional meteorology and, in turn, how these altered conditions impact fire activity.
- Uncertainty quantification: Our single-model approach does not explicitly account for model structural uncertainty, parameter sensitivity, or internal variability from ensemble simulations. While our study using CLM5 provides a controlled framework to isolate climate-driven fire responses, multi-model comparisons such as those conducted in the FireMIP initiative (Hantson et al., 2016; Teckentrup et al., 2019; Burton et al., 2024a) have shown that inter-model differences can lead to considerable spread in regional and global BA estimates. Additionally, Jones et al. (2022) demonstrated that uncertainty in fire emissions can stem from interactions between land cover change and fire suppression assumptions. Future studies should incorporate ensemble simulations or model intercomparison frameworks to more robustly assess projection uncertainty and guide policy-relevant interpretation.

## 5 Conclusions

This study demonstrates that boreal (NET) regions are likely to experience a marked intensification of wildfire activity under high-warming scenarios, driven by declining soil moisture and increasing vegetation carbon. These changes could transform boreal forests from carbon sinks into net carbon sources, amplifying global climate feedbacks. Despite uncertainties related to model structure and the exclusion of socioeconomic factors, the overall consistency between CLM5 simulations and observed fire-climate patterns supports the robustness of our results. Future work integrating land-use change, lightning variability, and sensitivity experiments will further refine projections of global fire activity. The broader implications of our findings extend to sustainable forest management and global climate policy. Balancing biomass harvesting with carbon sequestration goals will be crucial for maintaining ecosystem resilience. While afforestation and reforestation can enhance carbon storage, these efforts must be carefully designed in fire-prone regions to avoid unintentionally increasing fire risks. Adaptation strategies – such as fire-resilient afforestation, prioritization of fire-adapted species, ecosystem-appropriate fuel management, and development of early warning systems – will be essential to enhance resilience under future climate extremes. A comprehensive understanding of climate-fire-vegetation feedbacks is essential for developing robust adaptation and mitigation strategies that align with global sustainability objectives and effectively manage the compounded risks of future warming.

**Code availability.** The CLM5 model is publicly accessible through the Community Earth System Model repository (<https://github.com/ESCOMP/ctsm>, last access: 15 June 2024). The post-processing and visualization scripts used to analyze CLM5 output can be made available by the authors upon request.

**Data availability.** The input climate forcing datasets used to drive CLM5 are publicly available through the CESM/CMIP6 data repositories. The raw CLM5 simulation outputs generated in this study are very large (multiple terabytes) and therefore cannot be hosted in a public repository. These datasets can be made available by the authors upon request.

**Supplement.** The supplement related to this article is available online at <https://doi.org/10.5194/bg-22-7591-2025-supplement>.

**Author contributions.** HB: Writing – original draft, Methodology, Validation, Visualization, Formal analysis, conceptualization. MVM: Writing – review & editing, Validation, Formal analysis, Data curation. SS: Writing – review & editing. DHYY: Writing – review & editing, Formal analysis. APKT: Writing – review & editing.

ing, Validation, Supervision, Software, Methodology, Funding acquisition, conceptualization.

**Competing interests.** The contact author has declared that none of the authors has any competing interests.

**Disclaimer.** Publisher's note: Copernicus Publications remains neutral with regard to jurisdictional claims made in the text, published maps, institutional affiliations, or any other geographical representation in this paper. While Copernicus Publications makes every effort to include appropriate place names, the final responsibility lies with the authors. Views expressed in the text are those of the authors and do not necessarily reflect the views of the publisher.

**Acknowledgements.** This study is supported by an internal grant given to APKT by CUHK to support the CUHK-Exeter Joint Centre for Environmental Sustainability and Resilience (ENSURE; project no. 4930820). MVM acknowledges funding from the UKRI Future Leaders Fellowship Programme (MR/T019867/1). Part of the simulations were performed at the high-performance computing Cheyenne with the support provided by NCAR's Computational and Information Systems Laboratory, sponsored by the National Science Foundation (<https://doi.org/10.5065/D6RX99HX>). HB acknowledges the Research Grants Council (RGC) of Hong Kong for providing the Hong Kong PhD Fellowship Scheme 2020/21 (PF19-33279) and the HKSAR government for providing the Belt & Road scholarship.

**Financial support.** This research has been supported by the Chinese University of Hong Kong (grant no. 4930820) and the UK Research and Innovation (grant no. MR/T019867/1).

**Review statement.** This paper was edited by Mirco Migliavacca and reviewed by three anonymous referees.

## References

- Abatzoglou, J. T. and Williams, A. P.: Impact of anthropogenic climate change on wildfire across western US forests, *PNAS*, 113, 11770–11775, <https://doi.org/10.1073/pnas.1607171113>, 2016.
- Abatzoglou, J. T., Williams, A. P., and Barbero, R.: Global Emergence of Anthropogenic Climate Change in Fire Weather Indices, *Geophys. Res. Lett.*, 46, 326–336, <https://doi.org/10.1029/2018GL080959>, 2019.
- Aldersley, A., Murray, S. J., and Cornell, S. E.: Global and regional analysis of climate and human drivers of wildfire, *Sci. Total Environ.*, 409, 3472–3481, <https://doi.org/10.1016/j.scitotenv.2011.05.032>, 2011.
- Allen, R. J., Gomez, J., Horowitz, L. W., and Shevliakova, E.: Enhanced future vegetation growth with elevated carbon dioxide concentrations could increase fire activity, *Commun. Earth Environ.*, 5, <https://doi.org/10.1038/s43247-024-01228-7>, 2024.

- Andela, N., Morton, D. C., Giglio, L., Chen, Y., van der Werf, G. R., Kasibhatla, P. S., DeFries, R. S., Collatz, G. J., Hantson, S., Kloster, S., Bachelet, D., Forrest, M., Lasslop, G., Li, F., Mangen, S., Melton, J. R., Yue, C., and Randerson, J. T.: A human-driven decline in global burned area, *Science*, 356, 1356–1362, <https://doi.org/10.1126/science.aal4108>, 2017.
- Andreae, M. O. and Merlet, P.: Emission of trace gases and aerosols from biomass burning, *Global Biogeochem. Cycles*, 15, 955–966, <https://doi.org/10.1029/2000gb001382>, 2001.
- Bhattarai, H., Wu, G., Zheng, X., Zhu, H., Gao, S., Zhang, Y.-L., Widory, D., Ram, K., Chen, X., Wan, X., Pei, Q., Pan, Y., Kang, S., and Cong, Z.: Wildfire-Derived Nitrogen Aerosols Threaten the Fragile Ecosystem in Himalayas and Tibetan Plateau, *Environ. Sci. Technol.*, 57, 9243–9251, <https://doi.org/10.1021/acs.est.3c01541>, 2023.
- Bhattarai, H., Tai, A. P. K., Val Martin, M., and Yung, D. H. Y.: Impacts of changes in climate, land use, and emissions on global ozone air quality by mid-21st century following selected Shared Socioeconomic Pathways, *Sci. Total Environ.*, 906, 167759, <https://doi.org/10.1016/j.scitotenv.2023.167759>, 2024.
- Bondur, V. G., Mokhov, I. I., Voronova, O. S., and Sitnov, S. A.: Satellite Monitoring of Siberian Wildfires and Their Effects: Features of 2019 Anomalies and Trends of 20-Year Changes, *Dokl. Earth Sci.*, 492, 370–375, <https://doi.org/10.1134/s1028334x20050049>, 2020.
- Bowman, D. M., Balch, J. K., Artaxo, P., Bond, W. J., Carlson, J. M., Cochrane, M. A., D'Antonio, C. M., Defries, R. S., Doyle, J. C., Harrison, S. P., Johnston, F. H., Keeley, J. E., Krawchuk, M. A., Kull, C. A., Marston, J. B., Moritz, M. A., Prentice, I. C., Roos, C. I., Scott, A. C., Swetnam, T. W., van der Werf, G. R., and Pyne, S. J.: Fire in the Earth system, *Science*, 324, 481–484, <https://doi.org/10.1126/science.1163886>, 2009.
- Bowman, D. M. J. S., Kolden, C. A., Abatzoglou, J. T., Johnston, F. H., van der Werf, G. R., and Flannigan, M.: Vegetation fires in the Anthropocene, *Nature Reviews Earth & Environment*, 1, 500–515, <https://doi.org/10.1038/s43017-020-0085-3>, 2020.
- Burton, C., Lampe, S., Kelley, D. I., Thiery, W., Hantson, S., Christidis, N., Gudmundsson, L., Forrest, M., Burke, E., Chang, J., Huang, H., Ito, A., Kou-Giesbrecht, S., Lasslop, G., Li, W., Nieradzick, L., Li, F., Chen, Y., Randerson, J., Reyer, C. P. O., and Mengel, M.: Global burned area increasingly explained by climate change, *Nat. Clim. Change*, <https://doi.org/10.1038/s41558-024-02140-w>, 2024a.
- Burton, C. A., Kelley, D. I., Burke, E., Mathison, C., Jones, C. D., Betts, R. A., Robertson, E., Teixeira, J. C. M., Cardoso, M., and Anderson, L. O.: Fire weakens land carbon sinks before 1.5 °C, *Nat. Geosci.*, 17, 1108–1114, <https://doi.org/10.1038/s41561-024-01554-7>, 2024b.
- Byrne, B., Liu, J., Bowman, K. W., Pascolini-Campbell, M., Chatterjee, A., Pandey, S., Miyazaki, K., van der Werf, G. R., Wunch, D., Wennberg, P. O., Roehl, C. M., and Sinha, S.: Carbon emissions from the 2023 Canadian wildfires, *Nature*, <https://doi.org/10.1038/s41586-024-07878-z>, 2024.
- Cassell, B. A., Scheller, R. M., Lucash, M. S., Hurteau, M. D., and Loudermilk, E. L.: Widespread severe wildfires under climate change lead to increased forest homogeneity in dry mixed-conifer forests, *Ecosphere*, 10, e02934, <https://doi.org/10.1002/ecs2.2934>, 2019.
- Chen, Y., Hall, J., van Wees, D., Andela, N., Hantson, S., Giglio, L., van der Werf, G. R., Morton, D. C., and Randerson, J. T.: Multi-decadal trends and variability in burned area from the fifth version of the Global Fire Emissions Database (GFED5), *Earth Syst. Sci. Data*, 15, 5227–5259, <https://doi.org/10.5194/essd-15-5227-2023>, 2023a.
- Chen, Y., Hall, J., Wees, D., Andela, N., Hantson, S., Giglio, L., van der Werf, G., Morton, D., and Randerson, J.: Global Fire Emissions Database (GFED5) Burned Area (0.1), Zenodo [data set], <https://doi.org/10.5281/zenodo.7668424>, 2023b.
- Coen, J. L., Cameron, M., Michalak, J., Patton, E. G., Riggan, P. J., and Yedinak, K. M.: WRF-Fire: Coupled Weather–Wildland Fire Modeling with the Weather Research and Forecasting Model, *J. Appl. Meteorol. Climatol.*, 52, 16–38, <https://doi.org/10.1175/jamc-d-12-023.1>, 2013.
- Cunningham, C. X., Williamson, G. J., and Bowman, D. M. J. S.: Increasing frequency and intensity of the most extreme wildfires on Earth, *Nature Ecology & Evolution*, <https://doi.org/10.1038/s41559-024-02452-2>, 2024.
- Danabasoglu, G., Lamarque, J. F., Bacmeister, J., Bailey, D. A., DuVivier, A. K., Edwards, J., Emmons, L. K., Fasullo, J., Garcia, R., Gettelman, A., Hannay, C., Holland, M. M., Large, W. G., Lauritzen, P. H., Lawrence, D. M., Lenaerts, J. T. M., Lindsay, K., Lipscomb, W. H., Mills, M. J., Neale, R., Oleson, K. W., Otto-Bliesner, B., Phillips, A. S., Sacks, W., Tilmes, S., van Kampenhout, L., Vertenstein, M., Bertini, A., Dennis, J., Deser, C., Fischer, C., Fox-Kemper, B., Kay, J. E., Kinnison, D., Kushner, P. J., Larson, V. E., Long, M. C., Mickelson, S., Moore, J. K., Nienhouse, E., Polvani, L., Rasch, P. J., and Strand, W. G.: The Community Earth System Model Version 2 (CESM2), *J. Adv. Model. Earth Syst.*, 12, e2019MS001916, <https://doi.org/10.1029/2019MS001916>, 2020.
- Di Virgilio, G., Evans, J. P., Blake, S. A. P., Armstrong, M., Dowdy, A. J., Sharples, J., and McRae, R.: Climate Change Increases the Potential for Extreme Wildfires, *Geophys. Res. Lett.*, 46, 8517–8526, <https://doi.org/10.1029/2019gl083699>, 2019.
- Dong, C., Williams, A. P., Abatzoglou, J. T., Lin, K., Okin, G. S., Gillespie, T. W., Long, D., Lin, Y.-H., Hall, A., and MacDonald, G. M.: The season for large fires in Southern California is projected to lengthen in a changing climate, *Commun. Earth Environ.*, 3, <https://doi.org/10.1038/s43247-022-00344-6>, 2022.
- Fasullo, J. T., Otto-Bliesner, B. L., and Stevenson, S.: ENSO's Changing Influence on Temperature, Precipitation, and Wildfire in a Warming Climate, *Geophys. Res. Lett.*, 45, 9216–9225, <https://doi.org/10.1029/2018GL079022>, 2018.
- Flannigan, M. D., Krawchuk, M. A., de Groot, W. J., Wotton, B. M., and Gowman, L. M.: Implications of changing climate for global wildland fire, *Int. J. Wildland Fire*, 18, 483–507, <https://doi.org/10.1071/Wf08187>, 2009.
- Ford, B., Val Martin, M., Zelasky, S. E., Fischer, E. V., Anenberg, S. C., Heald, C. L., and Pierce, J. R.: Future Fire Impacts on Smoke Concentrations, Visibility, and Health in the Contiguous United States, *Geohealth*, 2, 229–247, <https://doi.org/10.1029/2018GH000144>, 2018.
- Forkel, M., Dorigo, W., Lasslop, G., Chuvieco, E., Hantson, S., Heil, A., Teubner, I., Thonicke, K., and Harrison, S. P.: Recent global and regional trends in burned area and their compensating environmental controls, *Environ. Res. Commun.*, 1, 051005, 2019.

- Fuller, D. O. and Murphy, K.: The Enso-Fire Dynamic in Insular Southeast Asia, *Clim. Change*, 74, 435–455, <https://doi.org/10.1007/s10584-006-0432-5>, 2006.
- Halofsky, J. E., Peterson, D. L., and Harvey, B. J.: Changing wildfire, changing forests: the effects of climate change on fire regimes and vegetation in the Pacific Northwest, USA, *Fire Ecol.*, 16, 4, <https://doi.org/10.1186/s42408-019-0062-8>, 2020.
- Hantson, S., Pueyo, S., and Chuvieco, E.: Global fire size distribution is driven by human impact and climate, *Global Ecol. Biogeogr.*, 24, 77–86, <https://doi.org/10.1111/geb.12246>, 2015.
- Hantson, S., Arneth, A., Harrison, S. P., Kelley, D. I., Prentice, I. C., Rabin, S. S., Archibald, S., Mouillot, F., Arnold, S. R., Artaxo, P., Bachelet, D., Ciais, P., Forrest, M., Friedlingstein, P., Hickler, T., Kaplan, J. O., Kloster, S., Knorr, W., Lasslop, G., Li, F., Mangeon, S., Melton, J. R., Meyn, A., Sitch, S., Spessa, A., van der Werf, G. R., Voulgarakis, A., and Yue, C.: The status and challenge of global fire modelling, *Biogeosciences*, 13, 3359–3375, <https://doi.org/10.5194/bg-13-3359-2016>, 2016.
- Hantson, S., Kelley, D. I., Arneth, A., Harrison, S. P., Archibald, S., Bachelet, D., Forrest, M., Hickler, T., Lasslop, G., Li, F., Mangeon, S., Melton, J. R., Nieradzik, L., Rabin, S. S., Prentice, I. C., Sheehan, T., Sitch, S., Teckentrup, L., Voulgarakis, A., and Yue, C.: Quantitative assessment of fire and vegetation properties in simulations with fire-enabled vegetation models from the Fire Model Intercomparison Project, *Geosci. Model Dev.*, 13, 3299–3318, <https://doi.org/10.5194/gmd-13-3299-2020>, 2020.
- Higuera, P. E. and Abatzoglou, J. T.: Record-setting climate enabled the extraordinary 2020 fire season in the western United States, *Global Change Biol.*, 27, 1–2, <https://doi.org/10.1111/gcb.15388>, 2021.
- IPCC: Climate Change 2014 – Impacts, Adaptation, and Vulnerability: Part A: Global and Sectoral Aspects, Contribution of Working Group II to the Fifth Assessment Report of the Intergovernmental Panel on Climate Change, Cambridge University Press, Cambridge, United Kingdom and New York, NY, USA, ISBN 9781107641655, 2014.
- Jolly, W. M., Cochrane, M. A., Freeborn, P. H., Holden, Z. A., Brown, T. J., Williamson, G. J., and Bowman, D. M.: Climate-induced variations in global wildfire danger from 1979 to 2013, *Nat. Commun.*, 6, 7537, <https://doi.org/10.1038/ncomms8537>, 2015.
- Jones, M. W., Abatzoglou, J. T., Veraverbeke, S., Andela, N., Lasslop, G., Forkel, M., Smith, A. J. P., Burton, C., Betts, R. A., van der Werf, G. R., Sitch, S., Canadell, J. G., Santín, C., Kolden, C., Doerr, S. H., and Le Quéré, C.: Global and Regional Trends and Drivers of Fire Under Climate Change, *Rev. Geophys.*, 60, e2020RG000726, <https://doi.org/10.1029/2020rg000726>, 2022.
- Jones, M. W., Veraverbeke, S., Andela, N., Doerr, S. H., Kolden, C., Mataveli, G., Pettinari, M. L., Le Quéré, C., Rosan, T. M., van der Werf, G. R., van Wees, D., and Abatzoglou, J. T.: Global rise in forest fire emissions linked to climate change in the extratropics, *Science*, 386, ead15889, <https://doi.org/10.1126/science.ad15889>, 2024.
- Kloster, S. and Lasslop, G.: Historical and future fire occurrence (1850 to 2100) simulated in CMIP5 Earth System Models, *Global Planet Change*, 150, 58–69, <https://doi.org/10.1016/j.gloplacha.2016.12.017>, 2017.
- Kloster, S., Mahowald, N. M., Randerson, J. T., and Lawrence, P. J.: The impacts of climate, land use, and demography on fires during the 21st century simulated by CLM-CN, *Biogeosciences*, 9, 509–525, <https://doi.org/10.5194/bg-9-509-2012>, 2012.
- Knorr, W., Jiang, L., and Arneth, A.: Climate, CO<sub>2</sub> and human population impacts on global wildfire emissions, *Biogeosciences*, 13, 267–282, <https://doi.org/10.5194/bg-13-267-2016>, 2016.
- Kochi, I., Donovan, G. H., Champ, P. A., and Loomis, J. B.: The economic cost of adverse health effects from wildfire-smoke exposure: a review, *Int. J. Wildland Fire*, 19, 803–817, <https://doi.org/10.1071/WF09077>, 2010.
- Lawrence, D. M., Fisher, R. A., Koven, C. D., Oleson, K. W., Swenson, S. C., Bonan, G., Collier, N., Ghimire, B., van Kampenhout, L., Kennedy, D., Kluzek, E., Lawrence, P. J., Li, F., Li, H. Y., Lombardozzi, D., Riley, W. J., Sacks, W. J., Shi, M. J., Vertenstein, M., Wieder, W. R., Xu, C. G., Ali, A. A., Badger, A. M., Bisht, G., van den Broeke, M., Brunke, M. A., Burns, S. P., Buzan, J., Clark, M., Craig, A., Dahlin, K., Drewniak, B., Fisher, J. B., Flanner, M., Fox, A. M., Gentine, P., Hoffman, F., Keppel-Aleks, G., Knox, R., Kumar, S., Lenaerts, J., Leung, L. R., Lipscomb, W. H., Lu, Y. Q., Pandey, A., Pelletier, J. D., Perket, J., Randerson, J. T., Ricciuto, D. M., Sanderson, B. M., Slater, A., Subin, Z. M., Tang, J. Y., Thomas, R. Q., Martin, M. V., and Zeng, X. B.: The Community Land Model Version 5: Description of New Features, Benchmarking, and Impact of Forcing Uncertainty, *J. Adv. Model. Earth Syst.*, 11, 4245–4287, <https://doi.org/10.1029/2018ms001583>, 2019.
- Li, F., Zeng, X. D., and Levis, S.: A process-based fire parameterization of intermediate complexity in a Dynamic Global Vegetation Model, *Biogeosciences*, 9, 2761–2780, <https://doi.org/10.5194/bg-9-2761-2012>, 2012.
- Li, F., Levis, S., and Ward, D. S.: Quantifying the role of fire in the Earth system – Part 1: Improved global fire modeling in the Community Earth System Model (CESM1), *Biogeosciences*, 10, 2293–2314, <https://doi.org/10.5194/bg-10-2293-2013>, 2013.
- Li, F., Lawrence, D. M., and Bond-Lamberty, B.: Impact of fire on global land surface air temperature and energy budget for the 20th century due to changes within ecosystems, *Environ. Res. Lett.*, 12, 044014, <https://doi.org/10.1088/1748-9326/aa6685>, 2017.
- Li, F., Val Martin, M., Andreae, M. O., Arneth, A., Hantson, S., Kaiser, J. W., Lasslop, G., Yue, C., Bachelet, D., Forrest, M., Kluzek, E., Liu, X., Mangeon, S., Melton, J. R., Ward, D. S., Darnenov, A., Hickler, T., Ichoku, C., Magi, B. I., Sitch, S., van der Werf, G. R., Wiedinmyer, C., and Rabin, S. S.: Historical (1700–2012) global multi-model estimates of the fire emissions from the Fire Modeling Intercomparison Project (FireMIP), *Atmos. Chem. Phys.*, 19, 12545–12567, <https://doi.org/10.5194/acp-19-12545-2019>, 2019.
- Li, F., Song, X., Harrison, S. P., Marlon, J. R., Lin, Z., Leung, L. R., Schwinger, J., Maréchal, V., Wang, S., Ward, D. S., Dong, X., Lee, H., Nieradzik, L., Rabin, S. S., and Séférian, R.: Evaluation of global fire simulations in CMIP6 Earth system models, *Geosci. Model Dev.*, 17, 8751–8771, <https://doi.org/10.5194/gmd-17-8751-2024>, 2024.
- Li, Y., Mickley, L. J., Liu, P., and Kaplan, J. O.: Trends and spatial shifts in lightning fires and smoke concentrations in response to 21st century climate over the national forests and parks of the western United States, *Atmos. Chem. Phys.*, 20, 8827–8838, <https://doi.org/10.5194/acp-20-8827-2020>, 2020.

- Liu, Y., Stanturf, J., and Goodrick, S.: Trends in global wildfire potential in a changing climate, *For. Ecol. Manage.*, 259, 685–697, <https://doi.org/10.1016/j.foreco.2009.09.002>, 2010.
- Liu, Y., Goodrick, S., and Heilman, W.: Wildland fire emissions, carbon, and climate: Wildfire–climate interactions, *For. Ecol. Manage.*, 317, 80–96, <https://doi.org/10.1016/j.foreco.2013.02.020>, 2014.
- Liu, Z., Ballantyne, A. P., and Cooper, L. A.: Biophysical feedback of global forest fires on surface temperature, *Nat. Commun.*, 10, 214, <https://doi.org/10.1038/s41467-018-08237-z>, 2019.
- Lizundia-Loiola, J., Otón, G., Ramo, R., and Chuvieco, E.: A spatio-temporal active-fire clustering approach for global burned area mapping at 250 m from MODIS data, *Remote Sens. Environ.*, 236, <https://doi.org/10.1016/j.rse.2019.111493>, 2020.
- Markewitz, D., Devine, S., Davidson, E. A., Brando, P., and Nepstad, D. C.: Soil moisture depletion under simulated drought in the Amazon: impacts on deep root uptake, *New Phytologist*, 187, 592–607, <https://doi.org/10.1111/j.1469-8137.2010.03391.x>, 2010.
- McCarty, J. L., Aalto, J., Paunu, V.-V., Arnold, S. R., Eckhardt, S., Klimont, Z., Fain, J. J., Evangeliou, N., Venäläinen, A., Tchepakova, N. M., Parfenova, E. I., Kupiainen, K., Soja, A. J., Huang, L., and Wilson, S.: Reviews and syntheses: Arctic fire regimes and emissions in the 21st century, *Biogeosciences*, 18, 5053–5083, <https://doi.org/10.5194/bg-18-5053-2021>, 2021.
- Muñoz Sabater, J.: ERA5-Land monthly averaged data from 1950 to present, Copernicus Climate Change Service (C3S) Climate Data Store (CDS) [data set], <https://doi.org/10.24381/cds.68d2bb30>, 2019.
- Nurrohmah, R. K., Kato, T., Ninomiya, H., Végh, L., Delbart, N., Miyauchi, T., Sato, H., Shiraishi, T., and Hirata, R.: Future projections of Siberian wildfire and aerosol emissions, *Biogeosciences*, 21, 4195–4227, <https://doi.org/10.5194/bg-21-4195-2024>, 2024.
- Owens, B.: Why are the Canadian wildfires so bad this year?, *Nature*, 618, 439–440, <https://doi.org/10.1038/d41586-023-01902-4>, 2023.
- Quilcaille, Y., Batibeniz, F., Ribeiro, A. F. S., Padrón, R. S., and Seneviratne, S. I.: Fire weather index data under historical and shared socioeconomic pathway projections in the 6th phase of the Coupled Model Intercomparison Project from 1850 to 2100, *Earth Syst. Sci. Data*, 15, 2153–2177, <https://doi.org/10.5194/essd-15-2153-2023>, 2023.
- Randerson, J. T., Van Der Werf, G. R., Giglio, L., Collatz, G. J., and Kasibhatla, P. S.: Global Fire Emissions Database, Version 4.1 (GFEDv4) [data set], <https://doi.org/10.3334/ORNLDAAAC/1293>, 2017.
- Roach, J.: Australia wildfire damages and losses to exceed \$100 billion, AccuWeather estimates, <https://www.accuweather.com/en/business/australia-wildfire-economic-damages-and-losses-to-reach-110-billion/657235> last access: 27 November 2023, 2020.
- Scholze, M., Knorr, W., Arnell, N. W., and Prentice, I. C.: A climate-change risk analysis for world ecosystems, *Proceedings of the National Academy of Sciences*, 103, 13116–13120, <https://doi.org/10.1073/pnas.0601816103>, 2006.
- Senande-Rivera, M., Insua-Costa, D., and Miguez-Macho, G.: Spatial and temporal expansion of global wildland fire activity in response to climate change, *Nat. Commun.*, 13, 1208, <https://doi.org/10.1038/s41467-022-28835-2>, 2022.
- Shi, K. and Touge, Y.: Characterization of global wildfire burned area spatiotemporal patterns and underlying climatic causes, *Sci. Rep.*, 12, 644, <https://doi.org/10.1038/s41598-021-04726-2>, 2022.
- Tang, W., Emmons, L. K., Buchholz, R. R., Wiedinmyer, C., Schwantes, R. H., He, C., Kumar, R., Pfister, G. G., Worden, H. M., and Hornbrook, R. S.: Effects of Fire Diurnal Variation and Plume Rise on US Air Quality During FIREX-AQ and WE-CAN Based on the Multi-Scale Infrastructure for Chemistry and Aerosols (MUSICA0), *J. Geophys. Res. Atmos.*, 127, e2022JD036650, <https://doi.org/10.1029/2022JD036650>, 2022.
- Tang, W., Tilmes, S., Lawrence, D. M., Li, F., He, C., Emmons, L. K., Buchholz, R. R., and Xia, L.: Impact of solar geoengineering on wildfires in the 21st century in CESM2/WACCM6, *Atmos. Chem. Phys.*, 23, 5467–5486, <https://doi.org/10.5194/acp-23-5467-2023>, 2023.
- Teckentrup, L., Harrison, S. P., Hantson, S., Heil, A., Melton, J. R., Forrest, M., Li, F., Yue, C., Arneth, A., Hickler, T., Sitch, S., and Lasslop, G.: Response of simulated burned area to historical changes in environmental and anthropogenic factors: a comparison of seven fire models, *Biogeosciences*, 16, 3883–3910, <https://doi.org/10.5194/bg-16-3883-2019>, 2019.
- Turco, M., von Hardenberg, J., AghaKouchak, A., Llasat, M. C., Provenzale, A., and Trigo, R. M.: On the key role of droughts in the dynamics of summer fires in Mediterranean Europe, *Sci. Rep.*, 7, 81, <https://doi.org/10.1038/s41598-017-00116-9>, 2017.
- Turco, M., Abatzoglou, J. T., Herrera, S., Zhuang, Y., Jerez, S., Lucas, D. D., AghaKouchak, A., and Cvijanovic, I.: Anthropogenic climate change impacts exacerbate summer forest fires in California, *Proceedings of the National Academy of Sciences*, 120, e2213815120, <https://doi.org/10.1073/pnas.2213815120>, 2023.
- Tymstra, C., Stocks, B. J., Cai, X., and Flannigan, M. D.: Wildfire management in Canada: Review, challenges and opportunities, *Prog. Disaster Sci.*, 5, 100045, <https://doi.org/10.1016/j.pdisas.2019.100045>, 2020.
- Val Martin, M., Heald, C. L., Lamarque, J.-F., Tilmes, S., Emmons, L. K., and Schichtel, B. A.: How emissions, climate, and land use change will impact mid-century air quality over the United States: a focus on effects at national parks, *Atmos. Chem. Phys.*, 15, 2805–2823, <https://doi.org/10.5194/acp-15-2805-2015>, 2015.
- van der Werf, G. R., Randerson, J. T., Giglio, L., Collatz, G. J., Mu, M., Kasibhatla, P. S., Morton, D. C., DeFries, R. S., Jin, Y., and van Leeuwen, T. T.: Global fire emissions and the contribution of deforestation, savanna, forest, agricultural, and peat fires (1997–2009), *Atmos. Chem. Phys.*, 10, 11707–11735, <https://doi.org/10.5194/acp-10-11707-2010>, 2010.
- Veira, A., Lasslop, G., and Kloster, S.: Wildfires in a warmer climate: Emission fluxes, emission heights, and black carbon concentrations in 2090–2099, *J. Geophys. Res.: Atmos.*, 121, 3195–3223, <https://doi.org/10.1002/2015jd024142>, 2016.
- Virkkala, A.-M., Rogers, B. M., Watts, J. D., Arndt, K. A., Potter, S., Wargowsky, I., Schuur, E. A. G., See, C. R., Mauritz, M., Boike, J., Bret-Harte, M. S., Burke, E. J., Burrell, A., Chae, N., Chatterjee, A., Chevallier, F., Christensen, T. R., Commene, R., Dolman, H., Edgar, C. W., Elberling, B., Emmerton, C. A., Euskirchen, E. S., Feng, L., Göckede, M., Grelle, A., Helbig, M.,



- Holl, D., Järveoja, J., Karsanaev, S. V., Kobayashi, H., Kutzbach, L., Liu, J., Luijkx, I. T., López-Blanco, E., Lunneberg, K., Mammarella, I., Marushchak, M. E., Mastepanov, M., Matsuura, Y., Maximov, T. C., Merbold, L., Meyer, G., Nilsson, M. B., Niwa, Y., Oechel, W., Palmer, P. I., Park, S.-J., Parmentier, F.-J. W., Peichl, M., Peters, W., Petrov, R., Quinton, W., Rödenbeck, C., Sachs, T., Schulze, C., Sonnentag, O., St. Louis, V. L., Tuitila, E.-S., Ueyama, M., Varlagin, A., Zona, D., and Natali, S. M.: Wildfires offset the increasing but spatially heterogeneous Arctic–boreal CO<sub>2</sub> uptake, *Nat. Clim. Change*, 15, 188–195, <https://doi.org/10.1038/s41558-024-02234-5>, 2025.
- Walker, A. P., De Kauwe, M. G., Bastos, A., Belmecheri, S., Georgiou, K., Keeling, R. F., McMahon, S. M., Medlyn, B. E., Moore, D. J. P., Norby, R. J., Zaehle, S., Anderson-Teixeira, K. J., Battipaglia, G., Brien, R. J. W., Cabugao, K. G., Cailleret, M., Campbell, E., Canadell, J. G., Ciais, P., Craig, M. E., Ellsworth, D. S., Farquhar, G. D., Fatichi, S., Fisher, J. B., Frank, D. C., Graven, H., Gu, L., Haverd, V., Heilmann, K., Heimann, M., Hungate, B. A., Iversen, C. M., Joos, F., Jiang, M., Keenan, T. F., Knauer, J., Korner, C., Leshyk, V. O., Leuzinger, S., Liu, Y., MacBean, N., Malhi, Y., McVicar, T. R., Penuelas, J., Pongratz, J., Powell, A. S., Riutta, T., Sabot, M. E. B., Schleucher, J., Sitch, S., Smith, W. K., Sulman, B., Taylor, B., Terrer, C., Torn, M. S., Treseder, K. K., Trugman, A. T., Trumbore, S. E., van Mantgem, P. J., Voelker, S. L., Whelan, M. E., and Zuidema, P. A.: Integrating the evidence for a terrestrial carbon sink caused by increasing atmospheric CO<sub>2</sub>, *New Phytol.*, 229, 2413–2445, <https://doi.org/10.1111/nph.16866>, 2021.
- Wright, H. E. and Heinselman, M. L.: The Ecological Role of Fire in Natural Conifer Forests of Western and Northern North America – Introduction, *Fire Ecol*, 10, 4–13, <https://doi.org/10.1007/BF03400628>, 2014.
- Wu, C., Venevsky, S., Sitch, S., Mercado, L. M., Huntingford, C., and Staver, A. C.: Historical and future global burned area with changing climate and human demography, *One Earth*, 4, 517–530, <https://doi.org/10.1016/j.oneear.2021.03.002>, 2021.
- Wu, C., Sitch, S., Huntingford, C., Mercado, L. M., Venevsky, S., Lasslop, G., Archibald, S., and Staver, A. C.: Reduced global fire activity due to human demography slows global warming by enhanced land carbon uptake, *Proceedings of the National Academy of Sciences*, 119, e2101186119, <https://doi.org/10.1073/pnas.2101186119>, 2022.
- Zhang, Y., Fan, J., Shrivastava, M., Homeyer, C. R., Wang, Y., and Seinfeld, J. H.: Notable impact of wildfires in the western United States on weather hazards in the central United States, *PNAS*, 119, e2207329119, <https://doi.org/10.1073/pnas.2207329119>, 2022.
- Zheng, B., Ciais, P., Chevallier, F., Chuvieco, E., Chen, Y., and Yang, H.: Increasing forest fire emissions despite the decline in global burned area, *Sci. Adv.*, 7, eabh2646, <https://doi.org/10.1126/sciadv.abh2646>, 2021.
- Zheng, B., Ciais, P., Chevallier, F., Yang, H., Canadell, J. G., Chen, Y., van der Velde, I. R., Aben, I., Chuvieco, E., and Davis, S. J.: Record-high CO<sub>2</sub> emissions from boreal fires in 2021, *Science*, 379, 912–917, <https://doi.org/10.1126/science.ade0805>, 2023.
- Zubkova, M., Humber, M. L., and Giglio, L.: Is global burned area declining due to cropland expansion? How much do we know based on remotely sensed data?, *Int. J. Remote Sens.*, 44, 1132–1150, <https://doi.org/10.1080/01431161.2023.2174389>, 2023.